CHALMERS
UNIVERSITY OF TECHNOLOGY

Optimal Steering Control of Long Combination Vehicle with Multiple Steered Units

Minimizing Swept Path Width, Off-Tracking and Rearward Amplification

Master's thesis in Mobility Engineering

KARTIK SHINGADE
SHREEKARA RAMESH

DEPARTMENT OF MECHANICS AND MARITIME SCIENCES

CHALMERS UNIVERSITY OF TECHNOLOGY
Gothenburg, Sweden 2024
www.chalmers.se

Master's thesis 2024

Optimal steering control of long combination vehicle with multiple steered units

Kartik Shingade
Shreekara Ramesh

CHALMERS
UNIVERSITY OF TECHNOLOGY

Department of Mechanics and Maritime Sciences
Chalmers University of Technology
Gothenburg, Sweden 2024

Optimal steering control of long combination vehicle with multiple steered units.

Supervisors:
Erdinc Umur, Volvo Group Trucks Technology
Sadeghi Maliheh Kati, Volvo Group Trucks Technology

Examiner:
Mats Jonasson, Mechanics & Maritime Sciences

Master's Thesis 2024
Department of Mechanics and Maritime Sciences
Division of Vehicle technology and autonomous systems
Chalmers University of Technology
SE-412 96 Gothenburg
Telephone +46 31 772 1000

Printed by Chalmers Reproservice
Gothenburg, Sweden 2024

Optimal Steering Control of Long Combination Vehicle with Multiple Steered Units.

KARTIK SHINGADE
SHREEKARA RAMESH
Department of Mechanics and Maritime Sciences
Chalmers University of Technology

Abstract

The introduction of Long Combination Vehicles (LCVs) with enhanced load-carrying capacities is a significant advancement in reducing carbon emissions and improving logistical efficiency. By decreasing the number of vehicles on the road, these LCVs contribute to a more sustainable and streamlined freight transport system. However, the increased length and load of these vehicles present challenges in maneuverability in tight spaces and lateral stability at high speeds. This research explores innovative solutions, such as multiple steered and propelled axles, which, when optimally controlled, address these challenges and enhance LCVs performance.
The primary focus of this thesis is the lateral dynamics of LCVs, specifically examining lateral off-tracking, swept path width, and rearward amplification. We utilize an A-double long combination vehicle equipped with two steerable and propelled axles as actuators. To improve maneuverability and lateral stability, we develop mathematical expressions for the aforementioned performance characteristics. These expressions serve as cost functions, which are minimized to determine the optimal control inputs for our actuators.
The optimization process is conducted using the CasADi toolbox in MATLAB, which provides a robust framework for defining the system dynamics and constraints necessary for the optimization problem. We evaluate the performance of the cost functions across various maneuvers and actuator configurations, highlighting the benefits of multiple actuators with optimal control allocation. The results demonstrate significant improvements in maneuverability at low speeds and lateral stability at high speeds, underscoring the potential of advanced control strategies in enhancing LCVs performance.

Keywords: Long Combination Vehicle, Optimal Control Allocation, Swept Path Width, Lateral Off-Tracking, Rearward Amplification, .

Acknowledgements

We would like to extend our heartfelt gratitude to our supervisor, Umur Erdinc, and our examiner, Mats Jonasson. Their professional expertise and unwavering enthusiasm have been invaluable throughout the entirety of our project.
We are also deeply appreciative of the Volvo Group's industrial supervisor, Maliheh Sadeghi, for providing us with this incredible opportunity and challenge. The comfortable environment and excellent facilities they offered significantly contributed to the successful completion of our project.
Additionally, we want to express our special thanks to our beloved friends and parents for their unwavering support and companionship. Their encouragement gave us the confidence to face the unknown and overcome difficulties, even in the most trying circumstances.

Kartik Shingade and Shreekara Ramesh, Gothenburg, August 2024

Nomenclature

Below is the nomenclature of indices, sets, parameters, and variables that have been used throughout this thesis.

Indices

i	vehicle unit number
j	instance in manuever

Parameters

m_1	mass of tractor (in kg)
m_2	mass of first trailer (in kg)
m_3	mass of dolly (in kg)
m_4	mass of second trailer (in kg)

Variables

X	x coordinate (in m) of CoG of tractor in global reference
Y	y coordinate (in m) of CoG of tractor in global reference
δ_1	Steering angle of tractor (in radian)
δ_2	Steering angle of dolly (in radian)
v_{1x}	Longitudinal velocity of tractor (in m/sec)
v_{1y}	Lateral velocity of tractor (in m/sec)
ϕ_1	Yaw angle of tractor (in radian)
$\dot{\phi}_1$	Yaw rate of tractor (radians/sec)
v_{2x}	Longitudinal velocity of first trailer (in m/sec)
v_{2y}	Lateral velocity of first trailer (in m/sec)

ϕ_2	Yaw angle of first trailer (in radian)
$\dot{\phi}_2$	Yaw rate of first trailer (in radians/sec)
v_{3x}	Longitudinal velocity of dolly (in m/sec)
v_{3y}	Lateral velocity of dolly (in m/sec)
ϕ_3	Yaw angle of dolly (in radian)
$\dot{\phi}_3$	Yaw rate of dolly (in radians/sec)
v_{4x}	Longitudinal velocity of second trailer (in m/sec)
v_{4y}	Lateral velocity of second trailer (in m/sec)
ϕ_4	Yaw angle of second trailer (in radian)
$\dot{\phi}_4$	Yaw rate of second trailer (in radians/sec)

Contents

List of Figures

1
Introduction

In this thesis, the control strategies for actuators in long combination vehicles (LCVs) are optimized to enhance maneuverability during tight corners and other demanding driving scenarios. This is crucial for ensuring safety and efficiency in the operation of these large, multi-trailer vehicles. To achieve this, two distinct vehicle models are employed: the kinematic model and the kinetic model.
The kinematic model simplifies the system by focusing on the geometric aspects of vehicle movement, disregarding forces and inertia. It is particularly useful for analyzing path tracking and low-speed maneuvers, where dynamic effects are minimal. On the other hand, the kinetic model or single track model incorporates the dynamics of the vehicle, including forces, torques, and the influence of mass distribution. This model is essential for understanding high-speed behaviors, stability, and the effects of external forces.
Both models are developed and analyzed in-depth to evaluate their respective advantages and limitations, using distinct cost functions based on the objective of optimization. Key performance metrics such as maneuverability, stability, and computational efficiency are considered. By simulating various driving scenarios, the models are compared and cost functions are evaluated to determine their effectiveness in real-time applications.
The comparative analysis aims to identify the most suitable model for practical implementation in LCVs. This involves assessing the trade-offs between the simplicity and computational efficiency of the kinematic model and the comprehensive, albeit more complex, kinetic model. The ultimate goal is to select a model that provides robust control while being feasible for real-time application, ensuring that LCVs can navigate tight corners and handle nervous situations with improved precision and safety.

1.1 Background

Transportation of goods is one of the key elements in maintaining the livelihood of any country's subjects and its economy. Road freight transport alone accounts for approximately 49.3% of all road transport in the European Union (EU) [1]. LCVs have the potential to significantly reduce CO2 emissions by approximately 24–38% [2] and operational costs by around 30–50%, compared to existing commercial vehicles. The increased capacity of LCVs compared to traditional commercial vehicles also suggests that, in the future, fewer LCVs (and their drivers) will be required to transport the same amount of cargo, potentially improving traffic fluidity on roads.

LCVs are vehicle combinations consisting of one prime-mover (truck or tractor) and multiple trailing units (such as trailers or semitrailers with dollies). One of the foremost challenges for LCVs are associated with their maneuverability at low speeds and stability at high speeds due to their increased length and number of articulations, which limits their rapid market introduction and penetration. However, the dolly presents an economically viable platform for addressing these challenges. This is mainly because it allows existing, unmodified semitrailers to remain in operation, which are the most frequently used trailing units in the EU, responsible for approximately 80–85% of cargo transportation [3].
The potential for dolly innovation can be comprehended from reducing swept path, off-tracking, rearward amplification and assist in power and reverse- parking. This paper specifically addresses the first 3 things by proposing an optimized dolly steering system using a single control structure and later adding propulsion on dolly. For demonstration purposes, a types of LCVs is considered: the A-double (i.e., tractor-semitrailer-dolly-semitrailer), which has the highest potential from an economic perspective.

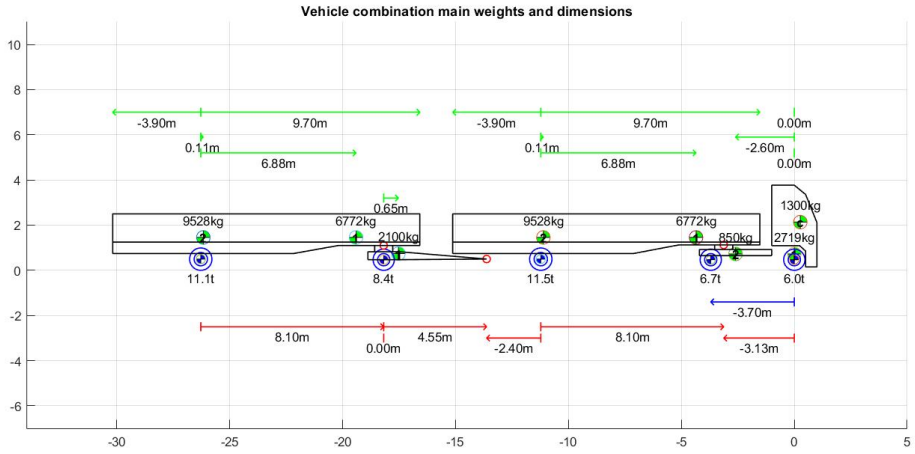

Figure 1.1: A-double combination configuration.

The Performance Based Standards (PBS) are used as measures for evaluating the performance enhancement of the considered LCVs due to the implementation of the steered dolly, compared to their conventional non-steered dolly versions. The PBS measures considered for low-speed maneuvers include swept path width and tail swing, while the PBS measures for high-speed performance include rearward amplification. To achieve this, both the most simplistic kinematic model and the single-track model are used for analysis. By comparing these models, the study aims

to identify the most effective control strategy for real-time application, ensuring enhanced maneuverability and stability of LCVs in various driving conditions.
The comprehensive analysis provided in this paper aims to demonstrate the benefits of optimized dolly steering and propulsion. It not only addresses the current limitations of LCVs in terms of maneuverability and stability but also paves the way for their broader adoption in the transport sector, ultimately contributing to environmental sustainability and operational efficiency.

1.2 Purpose

In this thesis, we aim to investigate the lateral dynamics of LCVs, focusing on the A-double configuration. The lateral dynamics characteristics of interest include the swept path width (SPW) at low speeds, rearward amplification (RWA), and lateral off-tracking at high speeds.

LCVs like the A-double, with steering and propulsion control primarily from the tractor, face challenges when maneuvering in tight spaces such as roundabouts and intersections. By adding additional steering and propulsion actuators to the trailing units (here dolly) of the LCV, these maneuverability challenges can be mitigated.

However, a new challenge arises in distributing control signals to these actuators optimally to achieve the desired objectives, whether maneuvering in tight spaces or preserving lateral stability at high speeds.

To address this, we employ an optimal control allocation approach to distribute control signals to the actuators on the LCV, aiming to achieve specific objectives. These objectives are formulated as mathematical cost functions, and by evaluating these cost functions, we determine the optimal control allocation.

To this end, we developed both kinematic and kinetic vehicle models with steerable tractor and dolly axles. The kinetic model also accounts for propulsion forces. Using these models, we set up an optimization problem with the CasADi toolbox for MATLAB, focusing on optimizing actuator inputs to enhance vehicle performance during various maneuvers.

1.3 Limitations of scope

In the course of this thesis, several limitations had to be taken into consideration for the sake of reducing the problem complexity and keeping the time frame of the project. These limitations have an impact on the overall optimization and real-time application of the proposed method for LCVs. These limitations are detailed below:

- Both kinematic and kinetic models are single-track bicycle models (Wheels on left and right are combined as a single wheel on axle midpoint).

- The kinematic model is valid for steady state conditions.
- The kinematic model assumes zero lateral velocity at the wheels i.e. zero side slip at the wheels.
- The kinematic model is more accurate for low speed maneuvers.
- In the kinetic model the tire model is considered to be linear.
- There is no longitudinal slip taken into consideration in the kinetic model.
- Optimization is restricted to minimizing swept path and yaw amplification.
- Most maneuvers used to test the model are low speed maneuvers almost attending steady state, except lane change.
- The optimization model has a short coming of real time application on any high fidelity vehicle model due to time constraint.

1.4 Research Questions

Here are the research questions that this thesis focuses on, which we aim to address by the conclusion of this work::

- What is the optimal control strategy to enhance maneuverability and lateral stability of LCVs in challenging situations?
- Which vehicle model performs best within this control strategy?
- How effective and robust are the cost functions used in optimal control for achieving the desired objectives in specific maneuvers?

1.5 Outline of Report

In the following pages, this report will delve into the theoretical understanding underpinning our study, providing a comprehensive overview of the key concepts and knowledge that form the basis of our work. This foundational theory will include a detailed examination of vehicle dynamics, the principles of the bicycle model. Following the theoretical framework, we will describe the methodology employed for building the models and optimizing the dolly steering system. The process of developing the kinematic and kinetic models using the bicycle model approach. We will outline the steps taken to parameterize the models based on realistic vehicle data. A step-by-step description of the optimization process, including the design

of the control algorithm, the application of optimization techniques, and the specific constraints considered. An overview of the simulation environment, including the software tools used (such as MATLAB) and the setup for virtual testing. The scenarios and driving maneuvers tested in the simulations will be detailed. The results section then will present the findings of our study, using various data visualizations to highlight key insights. A detailed evaluation of the optimized dolly steering system using PBSs. Key metrics such as swept path width. A comparison of the performance of the kinematic and kinetic models, discussing their respective strengths and weaknesses. Finally, we will conclude by summarizing the main findings of our study, discussing their implications, acknowledging any limitations, and offering recommendations for future research and practical applications

2
Vehicle Dynamics

To set up an optimization scenario for optimal control allocation of an A-double combination, an insight into the mathematical modelling and vehicle dynamics is needed to understand and take into consideration the impact of system dynamics on achieving a desired objective.

All the modelling process is carried out as per the standard coordinate system used for vehicle frame. This is a right hand coordinate system, fixed in the center of gravity of the vehicle and is originated from the definition in ISO 8855.

The models described in the following sections is only based on planar dynamics. This means that the only interesting motions are the longitudinal, lateral and yaw motion. The longitudinal motion is defined along the x-axis, the lateral motions along the y-axis, and the rotation around the z-axis is referred to as the yaw motion.

In addition to the model being restricted to the planar dynamics, resistive forces like aerodynamic and rolling resistances are neglected, the units are considered as rigid masses and the left and right wheels have equal steer angle. There are also several assumptions regarding the tire dynamics which are discussed later.

Two models were derived for the combination, the first one is a more simplistic kinematic model based on geometric relations and velocity and the second one a more complex kinetic model, which take into account forces acting on the combination. Both vehicle models are single-track bicycle models, where the left and right wheels of an axle are merged and represented as a single wheel. For the kinetic models, linear tire models are presented.

2.1 Vehicle Configuration

In this thesis, the combination used is an A-double with steerable e-dolly. As the name suggests this is a combination with double trailers with a tractor and e-dolly. The dolly, which is used to connect the second trailer with the first trailer is also considered to have a steerable and propelled axles. To simplify the modelling and optimisation, the axles on the every unit are lumped. Hence in the vehicle model being investigated, the combination has a total of 5 axles. Two axles for the tractor and one axle each for the two trailers and e-dolly.
The dimensions of the combination are preserved as it is, each trailer has a length of

40-foot which makes the total combination length to be 32.5 meters. The considered track width for the entire combination is 2.5 meters.

2.2 Kinematic Bicycle Model

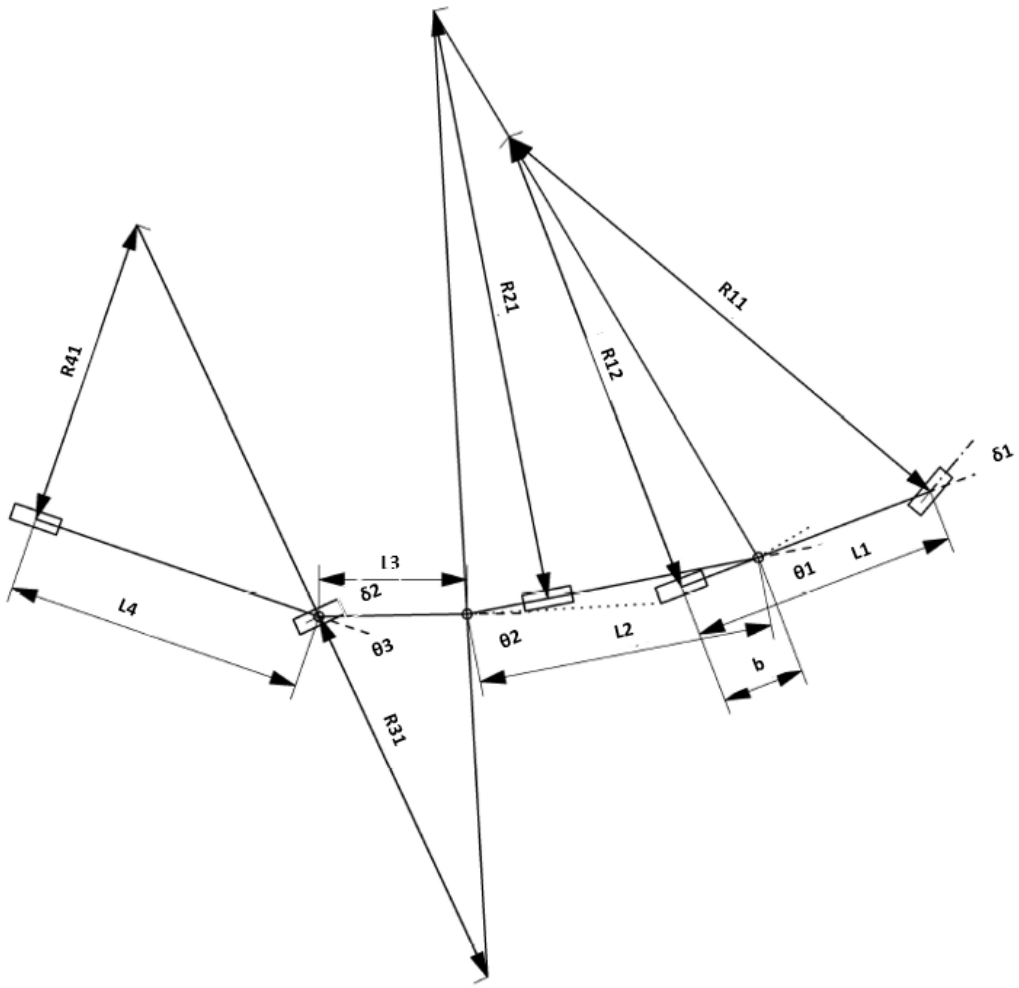

Figure 2.1: Kinematic model for A-double with steerable dolly.

The kinematic bicycle model is one of the simpler models of an A-double combination. This model is derived by following the approach of instantaneous centers, As shown in Figure 2.1 the motion of every unit of the combination can be broken down into rotation around an instantaneous center. These instantaneous centers are formed when perpendicular lines drawn from the velocity vectors of the axles intersect [4]. It is used to understand the geometric relations between several units of the vehicle in motion and to further simplify, an assumption is made that the center of gravity (CoG) of each unit is located at the midpoint of it's rear axle. Based on these geometric relations the equations for turning radius of every axle was derived as below.

The turning radius of the tractor's front axle is given by:

$$R_{11} = \sqrt{(R_{12}^2 + L_1^2)} \tag{2.1}$$

The turning radius of the tractor's rear axle is given by:

$$R_{12} = \frac{L_1}{\tan(\delta_1)} \tag{2.2}$$

The turning radius of first trailer's rear axle is given by:

$$R_{21} = \frac{L_2}{tan(\theta_1 + \beta_1)} \tag{2.3}$$

The turning radius of the dolly's axle is given by:

$$R_{31} = \frac{L_3(\cos(\beta_2 + \theta_2)}{sin(-\delta_2 + \beta_2 + \theta_2)} \tag{2.4}$$

The turning radius of the second trailer's rear axle is given by:

$$R_{41} = \frac{L_4}{\tan(\delta_2 + \theta_3)} \tag{2.5}$$

Further, in order use these equations in the optimisation problem, it is necessary to have time dependent equations. Since the radius of a unit can also be written as a ratio of longitudinal velocity to the yaw rate of that unit, the time dependent kinematic equations were obtained as below:

$$R_{ij} = \frac{V_{Xi}}{\phi_i}, \tag{2.6}$$

where R_{ij} is the turning radius of the jth axle of the ith unit, V_{xi} is the longitudinal velocity of that unit and ϕ_i is the yaw rate.

This approach can be extended to n number of units with n steerable axles. With the addition of steerable axle, the geometric relations change and the kinematic model needs to be reworked following the same principle of instantaneous centers.

The kinematic model has certain limitations. Firstly, it is only applicable for low-speed, steady-state maneuvers. Secondly, due to the low speed, the slip angle at the wheels is negligible. Lastly, this model does not take into account any forces acting on the vehicle.

2.3 Kinetic Bicycle Model

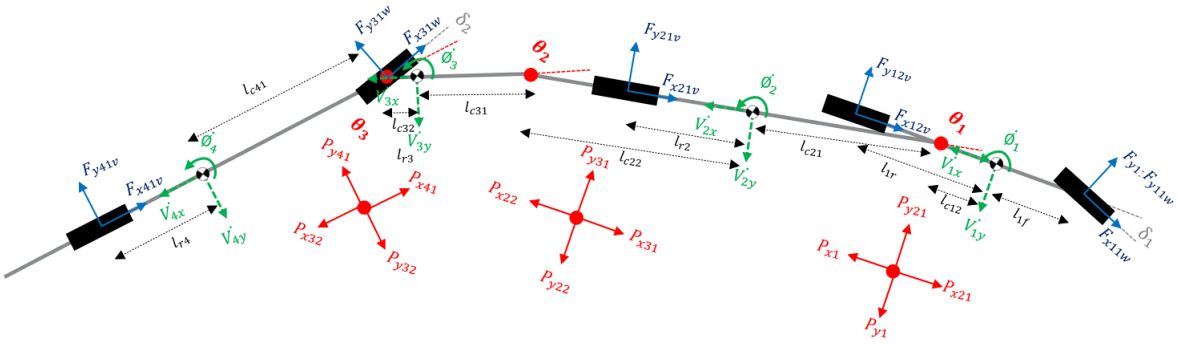

Figure 2.2: Kinetic bicycle model for A-double with steerable dolly.

The kinematic model is valid only for low-speed maneuvers. As speed increases, the model's accuracy diminishes due to the need to account for dynamic effects such as slip angles and forces acting on the vehicle combination. To address this, a single-track kinetic model was developed [5], as illustrated in Figure 2.2.

The equations of motion for this bicycle model are formulated using the Newtonian approach, which involves setting up force and moment balance equations for each unit in the combination. Since this model focuses solely on planar dynamics, roll and pitch motions are neglected. Consequently, each unit has three equations governing lateral force balance, longitudinal force balance, and moment balance along the z-axis. These equations can be solved using MATLAB's Symbolic Toolbox to obtain the desired explicit or implicit equations for the variables of interest in the optimization problem.

Below is the list of equations for the A-double combinations.

Equilibrium for tractor:

$$m_1\ (\dot{v}_{1x} - \dot{\phi}_1\ v_{1y}) = F_{x11w}\ cos(\delta_1) - F_{y11w}\ sin(\delta_1) + F_{x12v} - P_{x1} + P_{x21} \tag{2.7}$$

$$m_1\ (\dot{v}_{1y} + \dot{\phi}_1\ v_{1x}) = F_{x11w}\ sin(\delta_1) + F_{y11w}\ cos(\delta_1) + F_{y12v} - P_{y1} + P_{y21} \tag{2.8}$$

$$J_1\ \ddot{\phi}_1 = (sin(\delta_1)\ F_{x11w} + cos(\delta_1)\ F_{y11w})\ l_{1f} - F_{y12v}\ l_{1r} + P_{y1}\ l_{c12} - P_{y21}\ l_{c12} \tag{2.9}$$

Equilibrium for first trailer:

$$m_2\ (\dot{v}_{2x} - \dot{\phi}_2\ v_{2y}) = F_{x21v} + P_{x31} + P_{x21} - P_{x22} \tag{2.10}$$

$$m_2\ (\dot{v}_{2y} + \dot{\phi}_2\ v_{2x}) = F_{y21v} + P_{y31} + P_{y21} - P_{y22} \tag{2.11}$$

$$J_2\ \ddot{\phi}_2 = -F_{y21v}\ l_{2r} + P_{y22}\ l_{lc22} - P_{y31}\ l_{lc22} + P_{y21}\ l_{lc21} \tag{2.12}$$

Equilibrium for dolly:

$$m_3\ (\dot{v}_{3x} - \dot{\phi}_3\ v_{3y}) = F_{x31w}\ cos(\delta_2) - F_{y31w}\ sin(\delta_2) - P_{x41} + P_{x31} - P_{x32} \tag{2.13}$$

$$m_3\ (\dot{v}_{3y} + \dot{\phi}_3\ v_{3x}) = F_{x31w}\ sin(\delta_2) + F_{y31w}\ cos(\delta_2) - P_{y32} + P_{y41} + P_{y31} \tag{2.14}$$

$$J_3\ \ddot{\phi}_3 = -(sin(\delta_2)\ F_{x31w} + cos(\delta_2) F_{y31w})\ l_{3f} - P_{y41}\ l_{c32} + P_{y32}\ l_{c32} + P_{y31}\ l_{c31} \tag{2.15}$$

Equilibrium for second trailer:

$$m_4\ (\dot{v}_{4x} - \dot{\phi}_4\ v_{4y}) = F_{x41v} + P_{x41} - P_{x32} \tag{2.16}$$

$$m_4\ (\dot{v}_{4y} + \dot{\phi}_4\ v_{4x}) = F_{y41v} + P_{y41} - P_{y32} \tag{2.17}$$

$$J_4\ \ddot{\phi}_4 = -F_{y41v}\ l_{4r} + P_{y41}\ l_{lc41} - P_{y32}\ l_{lc41} \tag{2.18}$$

Coupling forces relations - coupling 1:

$$P_{x21} = -(P_{x1}\ cos(\theta_1) - P_{y1}\ sin(\theta_1)) \tag{2.19}$$

$$P_{y21} = -(P_{x1}\ sin(\theta_1) + P_{y1}\ sin(\theta_1)) \tag{2.20}$$

Coupling forces relations - coupling 2:

$$P_{x31} = -(P_{x22}\ cos(\theta_2) - P_{y22}\ sin(\theta_2)) \tag{2.21}$$

$$P_{y31} = -(P_{x22}\ sin(\theta_2) + P_{y22}\ sin(\theta_2)) \tag{2.22}$$

Coupling forces relations - coupling 3:

$$P_{x41} = -(P_{x32}\ cos(\theta_3) - P_{y32}\ sin(\theta_3)) \tag{2.23}$$

$$P_{y41} = -(P_{x32}\ sin(\theta_3) + P_{y32}\ sin(\theta_3)) \tag{2.24}$$

2.3.1 Tyre Model

A simplified tire model is employed for the above vehicle model [5], assuming the vehicle has a longitudinal slip-control onboard, it is not explicitly considered in the equations. For the lateral characteristic, the cornering stiffness is required to calculate the about of lateral force generated for a certain slip angle.

By using a fixed average value for cornering stiffness of tyre on either side of the axle, we assume a linear relationship between slip angle and lateral force. This assumption is effective for the small slip angles relevant to this study.

Linear tyre model for tractor:

$$s_{11y} = atan(v_{1yfw}/v_{1xfw}) \qquad s_{12y} = atan(v_{1yrv}/v_{1xrv}) \tag{2.25}$$

$$F_{y11w} = -C_{1f}\ s_{11y} \qquad F_{y12v} = -C_{1r}\ s_{12y} \tag{2.26}$$

Linear tyre model for first trailer:

$$s_{21y} = atan(v_{2yv}/v_{2xv}) \tag{2.27}$$

$$F_{y21v} = -C_{2r}\ s_{21y} \tag{2.28}$$

Linear tyre model for dolly:

$$s_{31y} = atan(v_{3yv}/v_{3xv}) \tag{2.29}$$

$$F_{y31v} = -C_{3r}\ s_{31y} \tag{2.30}$$

Linear tyre model for second trailer:

$$s_{41y} = atan(v_{4yv}/v_{4xv}) \tag{2.31}$$

$$F_{y41v} = -C_{4r}\ s_{41y} \tag{2.32}$$

There has to be compatibility equations which represents the velocity of other units with respect to tractor's as shown below the relations:

Velocity of tractor in vehicle-frame:

$$\begin{aligned} v_{1xfv} &= v_{1x} \\ v_{1yfv} &= v_{1y} + l_{1f}\ \dot{\phi}_1 \end{aligned} \tag{2.33}$$

$$\begin{aligned} v_{1xrv} &= v_{1x} \\ v_{1yrv} &= v_{1y} - l_{1r}\ \dot{\phi}_1 \end{aligned} \tag{2.34}$$

Velocity of tractor in wheel-frame:

$$\begin{aligned} v_{1xfw} &= v_{1xfv}\ cos(\delta_1) + v_{1yfv}\ sin(\delta_1) \\ v_{1yfw} &= v_{1yfv}\ cos(\delta_1) - v_{1xfv}\ sin(\delta_1) \end{aligned} \tag{2.35}$$

Velocity relation for coupling 01 (On-Tractor):

$$\begin{aligned} v_{1xc} &= v_{1xv} \\ v_{1yc} &= v_{1yv} - l_{c12}\ \dot{\phi}_1 \end{aligned} \tag{2.36}$$

Velocity relation for coupling 01 (On-Trailer):

$$\begin{aligned} v_{21xc} &= v_{1xc}\ cos(\theta_1) - v_{1yc}\ sin(\theta_1) \\ v_{21yc} &= v_{1yc}\ cos(\theta_1) + v_{1xc}\ sin(\theta_1) \end{aligned} \tag{2.37}$$

Velocity relation for first trailer CoG:

$$\begin{aligned} v_{2xv} &= v_{21xc} \\ v_{2yv} &= v_{21yc} - (l_{21c} + l_{2r})\dot{\phi}_2 \end{aligned} \tag{2.38}$$

Velocity relation for coupling 02 (on-trailer):

$$\begin{aligned} v_{22xc} &= v_{2xv} \\ v_{22yc} &= v_{2yv} - (l_{22c})\ \dot{\phi}_2 \end{aligned} \tag{2.39}$$

Velocity relation for coupling 02 (on-dolly):

$$\begin{aligned} v_{31xc} &= v_{22xc}\ cos(\theta_2) - v_{22yc}\ sin(\theta_2) \\ v_{31yc} &= v_{22yc}\ cos(\theta_2) + v_{22xc}\ sin(\theta_2) \end{aligned} \tag{2.40}$$

Velocity relation for dolly CoG:

$$\begin{aligned} v_{3xv} &= v_{31xc} \\ v_{3yv} &= v_{31yc} - (l_{31c} + l_{3r})\ \dot{\phi}_3 \end{aligned} \tag{2.41}$$

Velocity relation for coupling 03 (on-dolly):

$$\begin{aligned} v_{32xc} &= v_{3xv} \\ v_{32yc} &= v_{3yv} - (l_{32c})\ \dot{\phi}_3 \end{aligned} \tag{2.42}$$

Velocity relation for coupling 03 (on-trailer):

$$\begin{aligned} v_{41xc} &= v_{32xc}\ cos(\theta_3) - v_{32yc}\ sin(\theta_3) \\ v_{41yc} &= v_{32yc}\ cos(\theta_3) + v_{32xc}\ sin(\theta_3) \end{aligned} \tag{2.43}$$

Velocity relation for second trailer CoG:

$$\begin{aligned} v_{4xv} &= v_{41xc} \\ v_{4yv} &= v_{41yc} - (l_{41c} + l_{4r})\ \dot{\phi}_4 \end{aligned} \tag{2.44}$$

2.4 Vehicle Models Validation

In order to verify the above two models Volvo high fidelity model, Volvo Transport Model (VTM), was used. The methodology for which is quite simple convert both the models into state space form with carefully selecting states and input vector. Take the input and necessary states from the VTM, calculate the unknown states and their derivative and finally compare. For this, maneuver was circle of fixed radius of 25m, with vehicle running at constant low speed and road friction of 0.8, in order to achieve steady state.

2.4.1 Verification for Kinematic Model

A time based model was obtained using kinematic equations. Vehicle parameters and some sensor data like articulation angles, steering angle and tractor speed along the path (5m/sec)was taken from the VTM. These were used to calculate position, yaw rates and, longitudinal and lateral velocity of each units along the path.

The comparison below highlights the results from the VTM and the kinematic model for both steered and non-steered dolly in A-double combination. The plots in Figure 2.3 illustrate this comparison: the vehicle trajectory and the yaw rates of the individual units. The dotted line in the plots represents the actual data from the VTM, while the solid line corresponds to the kinematic model. The close resemblance between the two is striking, the maximum deviation in yaw rate that was noted in any unit of the combination was less than 3%. The reason for this similarity is straightforward: the kinematic model uses inputs derived from the VTM, and the maneuver is conducted at a steady state with very low vehicle velocity. If the speed is increased the effect of inertia and forces come into picture ruining the similarities.

2.4.2 Verification for Kinetic Model

The single track model described above needed verification against the VTM. To achieve this, similar sensor data and vehicle parameters were logged from the VTM too. The maneuver used for this verification was the same as the one used for the kinematic model verification, except for the radius of curvature, which was set to 30m in this case. Verifying the kinetic model required only a vehicle combination with a non-steered dolly, where an in-build path follower of VTM was used to perform a maneuver at constant speed (10m/sec) and constant steering angle. Subsequently, similar inputs was used for verification.

The comparison is illustrated through three different plots. Figure 2.4b demonstrates the kinetic model's ability to account for forces, showing results that closely align with the VTM. The other two plots, Figures 2.4a and 2.4c, highlight the strong performance of the single track model in comparison to the VTM during simpler maneuvers

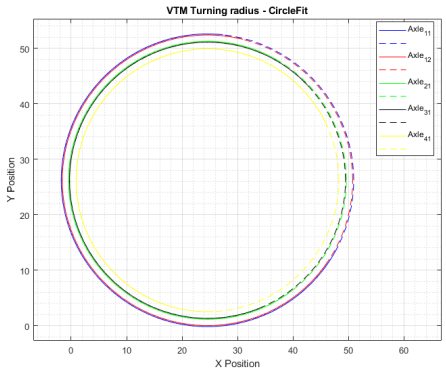

(a) Vehicle trajectory for non-steered dolly

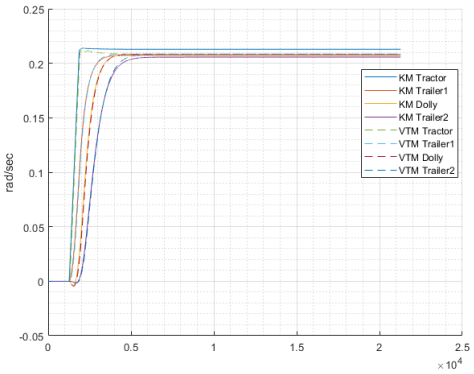

(b) Yaw rate of individual units for non-steered dolly

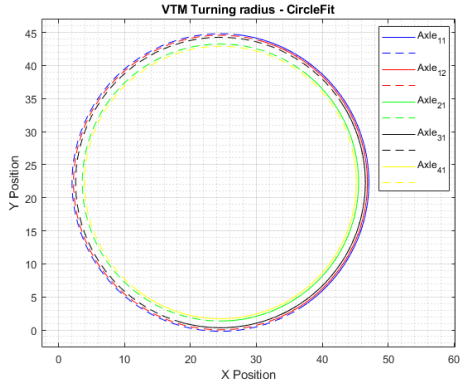

(c) Vehicle trajectory for steered dolly

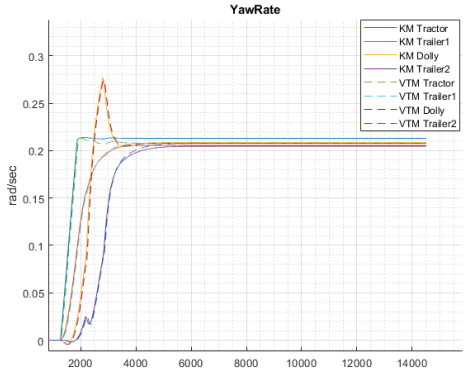

(d) Yaw rate of individual units steered dolly

Figure 2.3: Comparison between VTM and kinematic model for both non-steered and steered dolly in A-double combination

2.5 Performance Based Characteristics

The main criterion for determining if a vehicle should be allowed on the road is its performance and interaction with the road network. Performance-Based Characteristics (PBC) is one standard that assesses vehicle behavior both longitudinally and laterally. PBC evaluates how effectively and safely vehicles navigate various driving situations, such as turns, lane changes, and tight spaces [6]. LCVs, typically a truck tractor pulling multiple trailers, have increased overall length, impacting maneuverability, stability, and safety for both the vehicle and its surroundings. This thesis focuses specifically on the lateral performance of an A-double combination.

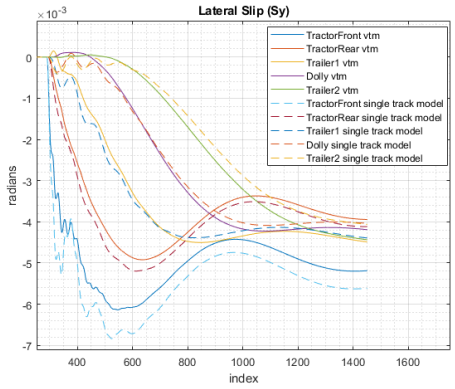

(a) Side slip angle at tyre

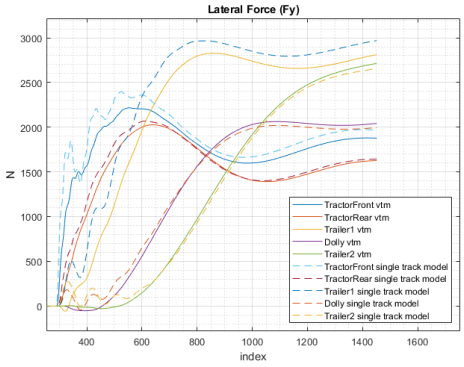

(b) Lateral force acting on the tyre

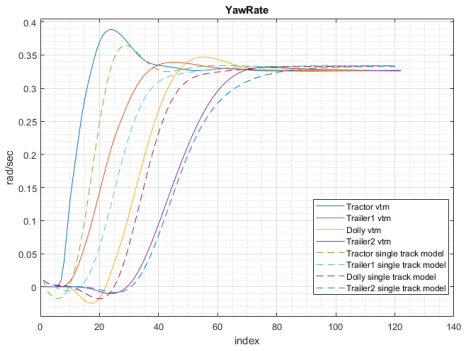

(c) Yaw rates of individual units

Figure 2.4: Comparison between VTM and Single track model for a non-steered dolly in A-double combination

2.5.1 Swept Path Width

The width of the swept path of a vehicle is a crucial parameter for comparing the performance of different articulated vehicle configurations. It measures the vehicle's ability to navigate roundabouts by indicating the maximum radial distance between the inner and outermost points of the vehicle's path when traveling around a curvature at low speed [5], as shown in Figure 2.5. This metric helps assess how well the vehicle can maneuver in tight, circular spaces, such as roundabouts.

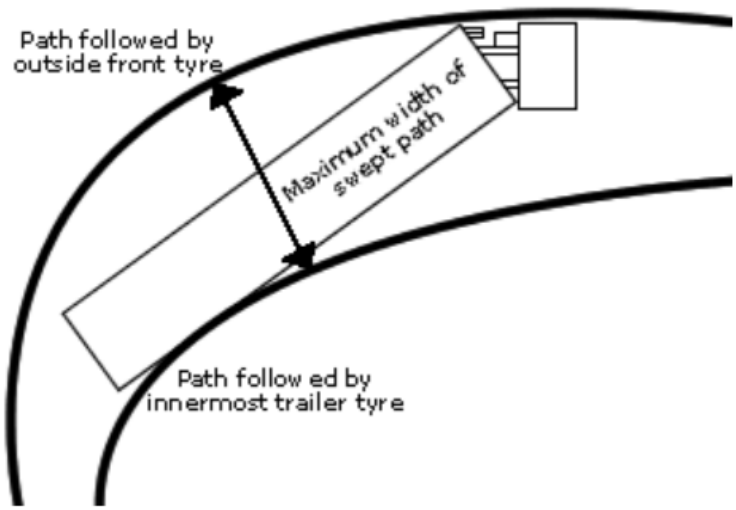

Figure 2.5: Swept Path Width measurement for a given vehicle

2.5.2 Low Speed Off-tracking

When an articulated commercial vehicle makes a turn at a low speed, the wheels of the rearmost trailer axle follows the path which is inside of the path of the tractor steering axle. This is called low speed off-tracking, as illustrated in Figure 2.6. It indicates the measure of swept path of the vehicle and its lateral road space requirement when the vehicle turns at 90 degree arc. The low speed off-tracking is measured as the maximum radial distance between the path of the midpoint of the steer axle and the path of the midpoint of the rearmost trailer axle.

2.5.3 High Speed Off-tracking

When an articulated commercial vehicle makes a steady turn at high speed, the rear of the truck tends to swing outward due to increased lateral acceleration. As the vehicle's speed increases, the low-speed off-tracking diminishes until the rearmost trailer axle follows the same path as the midpoint of the steer axle. At even higher speeds, the rearmost trailer axle begins to follow a path outside the steer axle's midpoint path. This phenomenon is known as high-speed off-tracking, and it is measured by the radial distance between the path of the midpoint of the steer axle and the path of the midpoint of the rearmost trailer axle, as depicted in Figure 2.7.

2.5.4 Rearward Amplification

When an LCV makes a sudden lateral movement, each unit in the combination experiences varying levels of lateral acceleration. This lateral acceleration increases progressively towards the rearmost unit of the vehicle, a phenomenon known as rearward amplification [7], as shown in Figure 2.8. Lower values of rearward amplification indicate better performance of the LCV, with an ideal rearward amplification

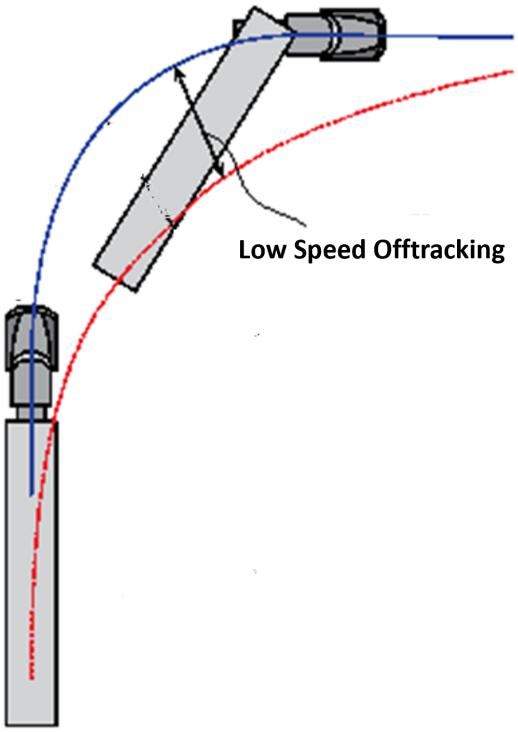

Figure 2.6: Lateral off-tracking at low speed

value being one, meaning there is no amplification of lateral acceleration from the front to the rear of the vehicle.

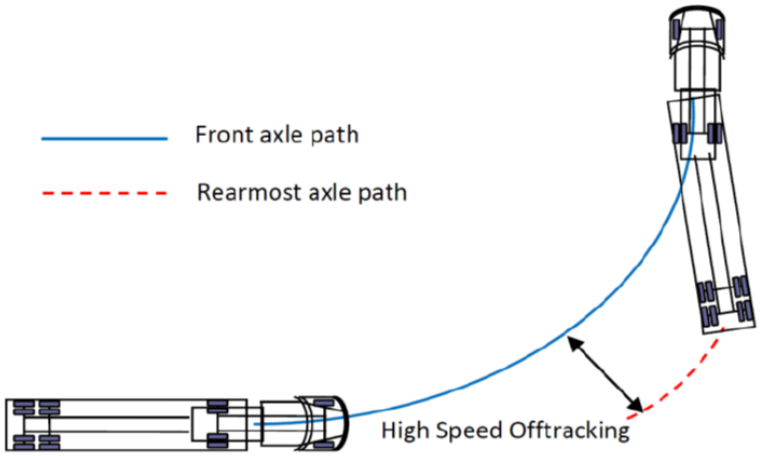

Figure 2.7: Lateral off-tracking distance at high speed

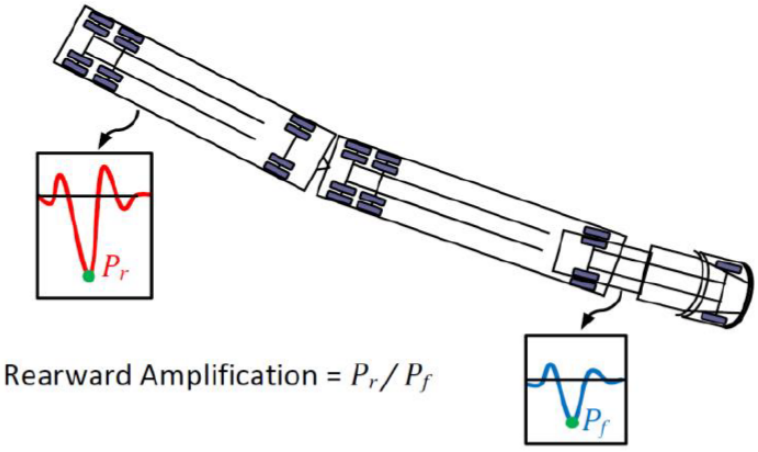

Figure 2.8: Rearward amplification of vehicle in terms of yaw rate (P_f and P_r)

3
Optimization

This chapter introduces the method for optimization, which can be loosely used for manual drive and automated drive. The overall optimization process is explained along with desired control allocations i.e propulsion and steering is optimized.

3.1 Optimal Control

Before getting into the process of optimization, it is crucial to understand why optimized control actions are necessary. Optimal control is the process of determining a control for a dynamic system such that a certain optimality criterion is achieved. This involves finding the best possible way to control a system to achieve desired outcomes while minimizing or maximizing specific performance measures [8]. This could lead to a system that is highly performance oriented and efficient while considering the factor of stability and safety.

3.2 Setting up Optimisation

The optimization scheme is broken down into several steps, which was carried out in symbolic tool for numerical optimization called CasADi. This is used for algorithmic differentiation and gradient based numerical optimization with strong focus on optimal control. One of the main advantages that it has is the use of the syntax of Computer Algebra Systems (CAS), allowing the user to construct symbolic expressions that can be differentiated in an efficient way using different algorithms for algorithmic differentiation.

3.2.1 System Dynamics

In order to define a system dynamics fixed set of inputs and state vector was chosen. This completely defines the system in explicit way, although being highly non-linear. Hence, the state space model for A-double is described below:

3.2.1.1 Kinematic System Dynamics

To define the system dynamics we need state variable and control actions. We assume that the tractor's CoG location is available from the GPS sensor data. Consequently, we can interpolate the positions of the other units behind the tractor, using their respective yaw angles too, which will be used in our later optimization

process. As a result state vector and control vector is defined as follows:

$$X = [X_1, Y_1, \phi_1, \phi_2, \phi_3, \phi_4] \tag{3.1}$$

$$U = [\delta_1, \delta_2] \tag{3.2}$$

where (X_1, Y_1) is the global coordinate of CG location of tractor and ϕ_i is the heading angle of respective units.

such that

$$\dot{X} = f(X, U) \tag{3.3}$$

has following representation in explicit form:

$$\dot{X_1} = v_{1x}\ cos(\phi_1) \tag{3.4}$$

$$\dot{Y_1} = v_{1x}\ sin(\phi_1) \tag{3.5}$$

$$\dot{\phi}_1 = v_{1x}/R_{11} \tag{3.6}$$

$$\dot{\phi}_2 = v_{2x}/R_{21} \tag{3.7}$$

$$\dot{\phi}_3 = v_{3x}/R_{31} \tag{3.8}$$

$$\dot{\phi}_4 = v_{4x}/R_{41} \tag{3.9}$$

Here, $\dot{\phi}_i$ is nothing but yaw rate of i_{th} unit.

3.2.1.2 Kinetic System Dynamics

Similar, to kinematic system dynamics, state variables of the model are

$$X = [X_1, Y_1, \phi_1, \phi_2, \phi_3, \phi_4, v_{1x}, v_{1y}, \dot{\phi}_1, \dot{\phi}_2, \dot{\phi}_3, \dot{\phi}_4] \tag{3.10}$$

While the control actions are

$$U = [F_{x12v}, \delta_1, \delta_2] \tag{3.11}$$

where, F_{x12v} is the traction force from rear axle of tractor.

3.2.1.3 Time to Path Distance Conversion

At low-speeds, a steering delay is required for dolly steering angles, otherwise tail swing increases. The steering delay for dolly rear axle is derived using geometric relation between axle position.
The system dynamics defined above is in time domain. Due to this the vehicle speeds are not allowed to vary during the turn especially stopping of the vehicle. However, in practical driving situations, e.g. sharp turns in parking lots etc., the driver often change the speeds and even could decide to stop the vehicle completely. Therefore it is important to formulate the problem in path distance domain. According to

[9] conversion from the time domain to the space domain can be performed by performing the following change of variables that results.

$$\frac{d(.)}{dt} = \frac{d(.)}{ds}\,\frac{ds}{dt} = v_{1x}\,\frac{d(.)}{ds} \tag{3.12}$$

and

$$\frac{d^2(.)}{dt^2} = \frac{d(.)}{dt}(\frac{d(.)}{ds}\,\frac{ds}{dt}) = {v_1}_x^2\,\frac{d^2(.)}{ds^2} + v_{1x}\,\frac{dv_{1x}}{ds}\,\frac{d(.)}{ds} \tag{3.13}$$

With this knowledge, the system dynamics for both the kinematic and kinetic models (as described in equations 3.2-3.8) were modified and subsequently utilized in the optimization process.

3.2.2 Initialization

To solve the nonlinear state space model integration is performed in accordance to the guess values. This also affects the optimization performance and efficiency. Since the optimisation is based on a receding horizon approach and we know the trajectory of the curve or maneuver. This helps in generating fairly accurate initial guess values for the optimal position and yaw angles of the vehicle. The state trajectory is discretized in to N intervals and system dynamics from equations are simulated using a Runge-Kutta integrator of order 4 (RK4) with a number of integration steps defined by 0.5m.

3.2.3 Constraints

Good constraints are essential to ensure the optimisation of the desired cost function is carried out within the realistic limitations of the actuators and also ensure the safe operation of the vehicle, not leading to unsafe modes such as jack-knifing or trailer swing. In order to ensure this, the major constraints limits on the steering wheel angle, articulation angle limits and also limit on the maximum force input based on the limit of the traction ellipse for every axle.

3.2.3.1 Kinematic Model Constraints:

Since the kinematic model doesn't involve any forces, the only actuation we have is with respect to the steering angles of the dolly and tractor. The constraints here are with respect to the initial and final positions and angles of the tractor, to ensure the optimisation begins from a desired state. The steering angles of the tractor and dolly axles are also limited to a range of steering wheel angle that is achievable in real life.

3.2.3.2 Kinetic Model Constraints:

With the inclusion of wheel forces in the kinetic model, it becomes to critical to ensure the optimisation follows the traction limits of the tire and hence a constraint is added such that the ability of generating longitudinal and lateral forces at the contact patches for every axle respects the traction ellipse.

3.2.4 Cost Function

Using all the state variables and inputs defined above and knowing the co-ordinates of our reference path we are able to define a mathematical expression, which when minimised at every instance in a maneuver leads to the minimisation of our desired characteristic, which in our case is:

- Objective 1 : Swept path minimization at low speed.
- Objective 2 : Minimization of high speed off-tracking.
- Objective 3 : Minimization of rearward amplification.

The expression used for achieving different objectives is the cost function, the cost function can be formulated in multiple ways. Here we explore four different ways of formulating the cost function and then compare their performances. In the cost function, we have two parts one part of the cost function gives us the cost of state deviation and the second part gives us the cost of the controlled input.

The cost of deviation follows an infinity norm constraint that is a variable is assigned with an inequality constraint on the state deviation, which limit the maximum absolute value of state deviation, this basically helps optimization to ensure that no single variable dominates the solution.

3.2.4.1 Cost Function 1: Tractor following approach

This cost function was formulated to replicate a manual driving scenario, where the tractor is controlled by a steering input from the driver. In this scenario the midpoint of the axle (when kinematic model is used) or CoG of the tractor (when kinetic model is used) is used as the reference trajectory for the following units. The cost function is then designed to penalise the deviation of the following units from the reference trajectory i.e. the path traced by the axle midpoint or CoG of tractor.

If the path traced by the axle mid point or CoG of the tractor is given by $(X_{tractor}, Y_{tractor})$ and the position of the following unit's CoG is given by (X_i, Y_i). The deviation e of the following unit from the reference path is calculated accounting for the delay in travelled distance (meaning when both tractor and trailing unit would have been on same location):

$$e_i = ((X_{tractor} - X_i)\ sin(\phi_i) + (Y_{tractor} - Y_i)\ cos(\phi_i))^2 \tag{3.14}$$

such that $e_i < r_{ot}$, where, r_{ot} is the infinity norm variable and $i = 1, 2, 3$ refers to the first trailer, the dolly, and the second trailer, respectively. The cost function is then given by:

$$F = w_1\ \sum(r_{ot}) + w_2\ \sum(U) \tag{3.15}$$

where, w_1, w_2 are weight penalization and,
$U = [\delta_1, \delta_2, F_{x12v}]^T$or $[\delta_1, \delta_2]^T$, depending on the vehicle model used.

3.2.4.2 Cost Function 2: Minimizing the deviation of Axle mid-point.

This cost function is aimed more towards autonomous or semi-autonomous driving application, where the control allocator also assigns values to the tractor steering. In this case, the system has trajectory information and from this reference coordinates are generated. The cost function penalises the deviation of axle mid point from this reference path.
In this scenario, the reference coordinates of the path is given by (X_{path}, Y_{path}) and the position of the axle mid points is given by (X_i, Y_i). The deviation e of the following unit from the reference path is calculated accounting for the delay in travelled distance:

$$e_i = ((X_{path} - X_i)\ sin(\phi_i) + (Y_{path} - Y_i)\ cos(\phi_i))^2 \quad \text{such that} \quad e_i < r_{ot} \tag{3.16}$$

where, r_{ot} is infinity norm variable and i = 1,2,3,4 refers to the tractor, the first trailer, the dolly and the second trailer, respectively. The cost function is then given by:

$$F = w_1 \sum(r_{ot}) + w_2 \sum(U) \tag{3.17}$$

where, again w_1, w_2 are weight penalization and,
$U = [\delta_1, \delta_2, F_{x12v}]^T$or $[\delta_1, \delta_2]^T$, depending on the vehicle model used.

3.2.4.3 Cost Function 3: Body corner deviations

This cost function tries to implement the definition of a swept path i.e. the distance between the inner and outer extremities of the vehicle while travelling through a corner. In multi-unit vehicle with multiple actuators, there is a possibility that any of the leading or trailing corner of every unit could form the outer most boundaries of the swept path. Hence, an array of distances is calculated from the the leading edge of the tractor's inner and outer corners to the leading and trailing edges of the following units as shown in the image below.

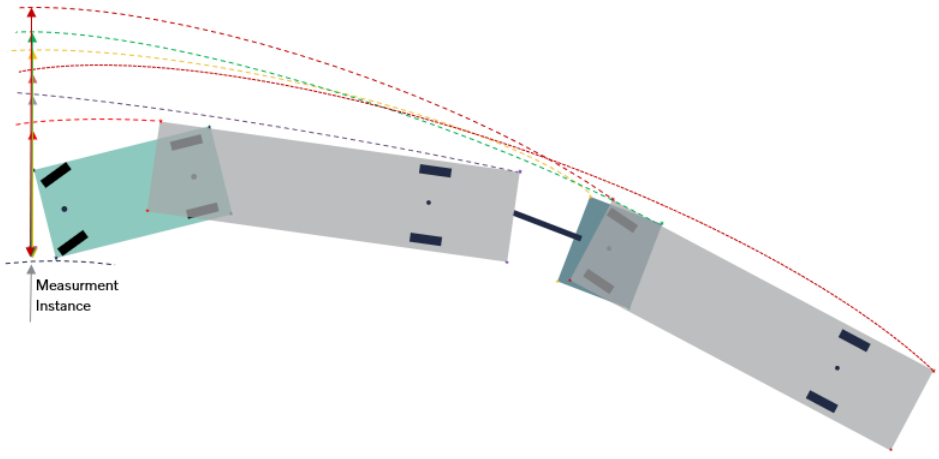

Figure 3.1: Calculation of swept path in body point cost function.

If $(X_{tractor_{in}}, Y_{tractorin})$ and $(X_{tractor_{out}}, Y_{tractorout})$ are the leading edges of the tractor body on the inner and outer sides - say left and right. And the inner and outer leading and trailing edges of the following units is given by $(X_{i_{in}}, Y_{iin})$ and $(X_{i_{out}}, Y_{iout})$ respectively.

The swept path measurement from the inner side of the tractor is given by:

$$SP_{in} = ((X_{tractor_{in}} - X_{i_{out}})\ sin(\phi_i) + (Y_{tractor_{in}} - Y_{i_{out}})\ cos(\phi_i))^2 \quad \text{such that} \quad SP_{in} < r_{ot1} \tag{3.18}$$

where, r_{ot1} is infinity norm variable
and $i = 1, 2, 3$ refers to the first trailer, the dolly, and the second trailer, respectively.
The swept path measurement from the outer side of the tractor is given by:

$$SP_{out} = ((X_{tractor_{out}} - X_{i_{in}})\ sin(\phi_i) + (Y_{tractor_{out}} - Y_{i_{in}})\ cos(\phi_i))^2 \quad \text{such that} \quad SP_{out} < r_{ot2} \tag{3.19}$$

where, r_{ot2} is another infinity norm variable
Finally, the cost function is then given by:

$$F = w_1\ \sum(r_{ot1}) + w_2\ \sum(r_{ot2}) + w_3\ \sum(U) \tag{3.20}$$

where, w_1, w_2, w_3 are weight penalization and, $U = [\delta_1, \delta_2, F_{x12v}]^T$or $[\delta_1, \delta_2]^T$, depending on the vehicle model used.

3.2.4.4 Cost Function 4: Yaw Amplification

This cost function is build to achieve the objective of minimising rearward amplification. As the definition of rearward amplification suggests its basically the ratio of maximum yaw rate of rearmost unit to maximum yaw rate of tractor. But here instead of ratio we take subtraction in order to avoid the possibility of an in-feasibility during optimization.

$$F = w_1\ \sum(e) + w_2\ \sum(U) \tag{3.21}$$

where, $e_j = \dot{\phi}_{4j} - \dot{\phi}_{1j}$ for j_{th} instance and,
$U = [\delta_1, \delta_2, F_{x12v}]^T$

3.2.5 Solution finding or Solver formulation

An NLP solver for CasADi is a vector that takes inputs and state vector with initial guesses for the solution and returns the optimal solution. The most popular NLP solver used in CasADi is IPOPT. Interior Point OPTimizer is a nonlinear optimization algorithm designed to deal with large-scale nonlinear programs. It is an open-source optimization algorithm that uses a interior-point line search filter method. IPOPT allows both objective function and constraints to be nonlinear and non convex as long as all functions are twice continuously differentiable. IPOPT is more accurate then sequential programs since it directly evaluates the nonlinear functions rather then linear or quadratic approximations [10].

3.3 Performance Assessment Maneuvers

To evaluate the performance of cost functions in different maneuvering scenarios, the most common road curvatures which challenge maneuverability in long combination vehicle were chosen as follows based on PBS [11].

- 180 degree roundabout maneuver :
  In order to evaluate the swept path and off-tracking at relatively high speed, this particular maneuver was chosen, which also represents the good characteristic of steady state. The radius of curve is set to be 30m with friction of 0.8 and vehicle is made to run at 10 km/hr and 40 km/hr to assess swept path and off tracking respectively.
- 90 degree turning maneuver:
  From Performance Based Characteristic test, the maneuver was obtained to access the A double combination for better performance in terms of swept path at tight corner negotiation at low speed of 10 km/hr and high speed off tracking for radius of 100 m at vehicle speed 75 km/hr.
- S-Curve turning maneuver:
  This curve specifically tests the swept path and steering effort from the driver, to compensate for very short steering input interval change with respect to tighter turn in opposite direction. This curve is evaluated for low speeds of 10km/hr and turning radius in both directions are 20 m.
- Single and double lane change:
  The lane change maneuvers are used to assess the rearward amplification of the LCV while travelling at high speed of 80 km/hr. These kind of maneuvers are usually seen at high speeds during overtaking and obstacle avoidance.

4

Simulation Results

Using above described cost functions, the lateral performance of A-double combination was assessed for given maneuvers. The optimization was done using both the models that is kinematic and Single track model, which also gives a scope to compare between two. Originally, the results depicts the improvement on performance in terms of swept path, off tracking and rearward amplification using active steerable dolly. Further the cost of computation and the robustness of model is evaluated in very crude manner.

4.1 Objective 1 Reflection - Minimizing Swept Path Width

4.1.1 Kinematic Results

In order to appreciate the benefit of an optimally steered dolly in reducing the swept path width for a given maneuver, it is essential to know the swept path for the combination in the same maneuver without a steerable dolly. This case of vehicle combination with no active steerable dolly is used a baseline. In this case only the tractor is made to follow a certain reference path, without any actuation in the following units. These results are then used to compare the swept path width results obtained by allocating optimal steering angle for the dolly based on the evaluation of different cost functions stated above.

4.1.1.1 180-Degree Turn

The plots in Figure 4.1 show the steering angles for the tractor and dolly and the trajectory of the vehicle combination. This is the base line case, where we have no dolly steering and as a result it can be seen the last unit of the combination has a very high lateral deviation from the path traced by the tractor resulting in a higher swept path. Figures 4.2 to 4.4 depict the steering angles for the tractor and dolly along with the resulting trajectories of the combination for different cost function evaluations.

4.1.1.2 No Dolly Steering

For this baseline case, the combination goes about the 180 degree curve which has a radius of 30m as mentioned earlier, at a constant low speed of 10 m/s. For this

maneuver without dolly steering, the combination's maximum swept path width came up to 5.3m.

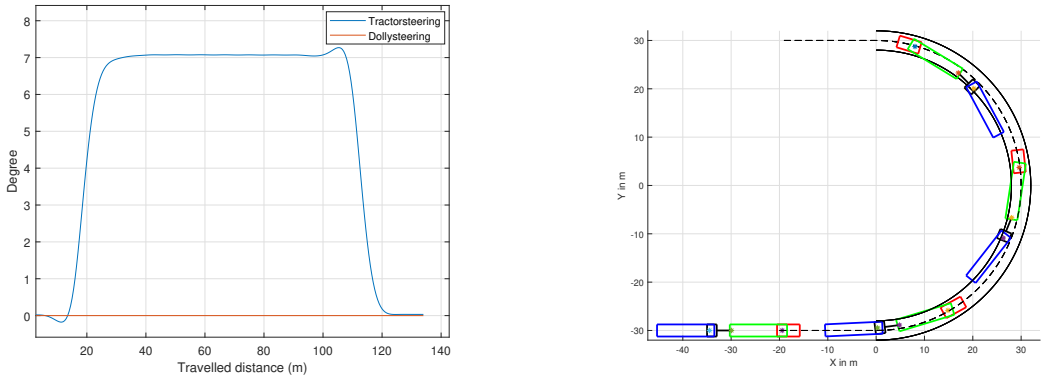

(a) Steering control input **(b)** Vehicle trajectory

Figure 4.1: Control inputs and trajectory of vehcile without optimization

4.1.1.3 Dolly Steering - Tractor Following Cost Function

By comparing Figure 4.2 with Figure 4.1, it can be seen the lateral deviation of the last trailer has reduced with the allocation of an optimal steering angle for the dolly. The characteristics of the maneuver and vehicle speed remain the same and the maximum swept path width was reduced to 3.85m

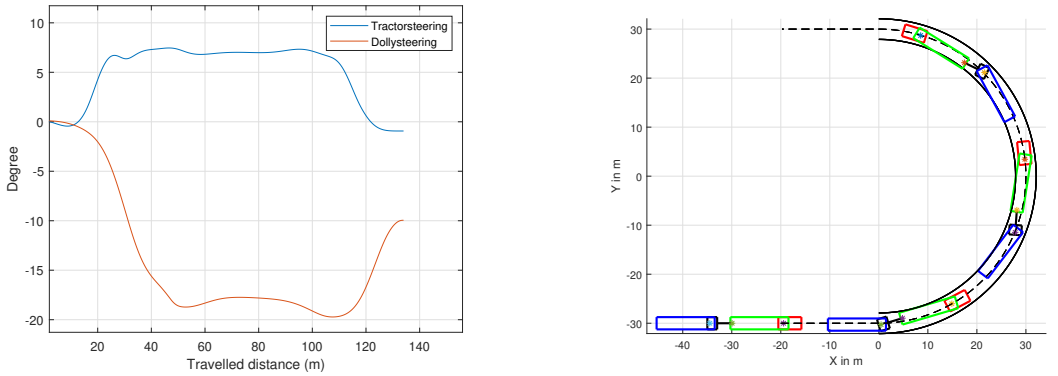

(a) Steering control input **(b)** Vehicle trajectory

Figure 4.2: Optimal control inputs and trajectory of vehicle using cost function 1

4.1.1.4 Dolly Steering - Axle Mid-Point Cost Function

In figure 4.3, we observe the performance of the axle mid-point cost function in reducing the swept path width during a 180-degree curve maneuver. In both figures 4.1b and 4.3b, the LVC undergoes the exact same maneuver. It is evident that the cost function effectively reduces the deviation of the trailing units in the latter case, keeping them well within the road boundaries. This is not the case in the former, where there is no steered dolly. While the effectiveness of this cost function is not as

significant as the previous tractor-following cost function, it still managed to reduce the maximum swept path width to 3.99 meters.

A notable advantage of the axle mid-point cost function can be seen in the actuator performance. By comparing the plots in Figure 4.2a and 4.3a, we observe that the input dynamics under the axle mid-point cost function are significantly more refined, with fewer fluctuations and smoother transitions. This improvement suggests a more controlled and efficient steering response.

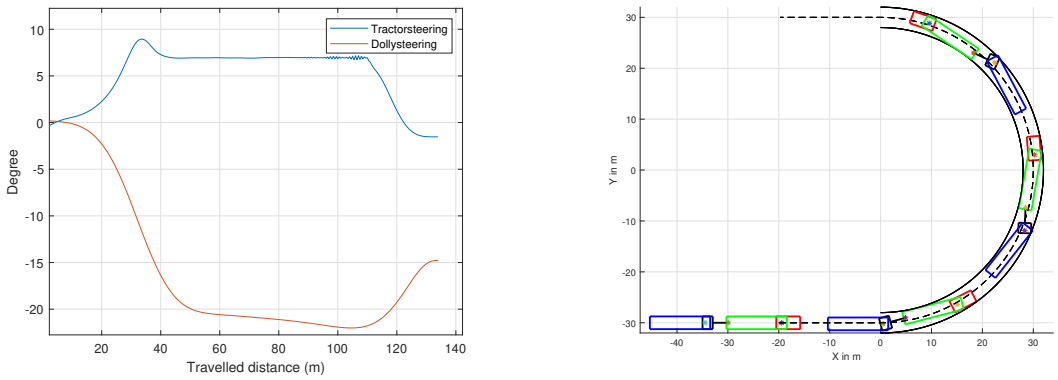

(a) Steering control input **(b)** Vehicle trajectory

Figure 4.3: Optimal control inputs and trajectory of vehicle using cost function 2

4.1.1.5 Dolly Steering - Body Corner Cost Function

The performance of the body corner cost function in reducing swept path width closely mirrors that of the tractor-following cost function, achieving a reduced swept path of 3.84 meters, as previously noted. From the trajectory plots in Figures 4.2b, 4.3b, and 4.4b, it's evident that the articulation angles of the LCV are significantly more aggressive with the axle mid-point cost function compared to the other two approaches, particularly as the vehicle approaches the midpoint of the corner. This is clearly visible in the third instance of the LCV from the trajectory plot. While this aggressive articulation effectively minimizes the deviation of the first trailer, it has minimal impact on further reducing the overall swept path width.

Investigating the actuator dynamics, we observe that the gradient of the steering inputs in Figure 4.4a is quite similar to that in Figure 4.2a. However, one notable improvement in the body corner cost function is the elimination of fluctuations that were present in the tractor-following cost function. This comparison is made under similar maneuver conditions, with comparable weightages assigned to state deviations and input penalties across the different cost functions.

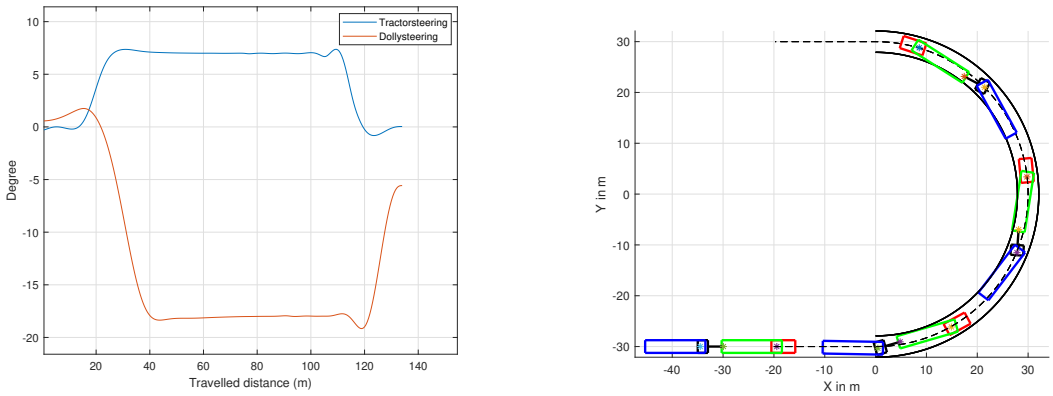

(a) Steering control input **(b)** Vehicle trajectory

Figure 4.4: Control inputs and trajectory for vehicle using cost function 3

4.1.1.6 Summary of Kinematic Results

By following the above steps, the evaluation of the cost functions for low speeds using the kinematic model was carried out for different maneuvers and the summary of their performance in reducing the swept path is presented in Figures from 4.5 to 4.7.

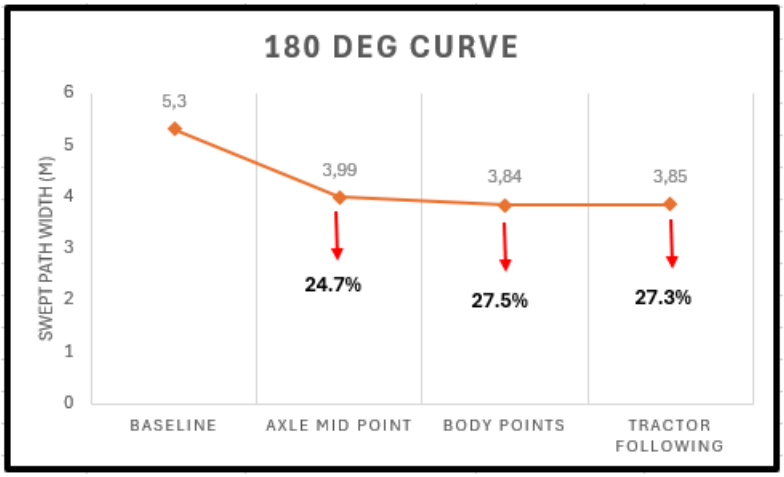

Figure 4.5: Performance of cost functions for a 180 deg. turn of radius 30m.

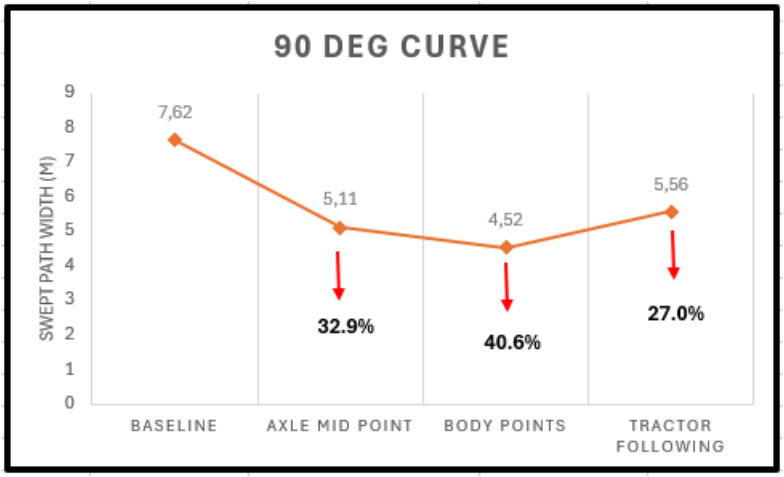

Figure 4.6: Performance of cost functions for a 90 deg. turn of radius 12.5m.

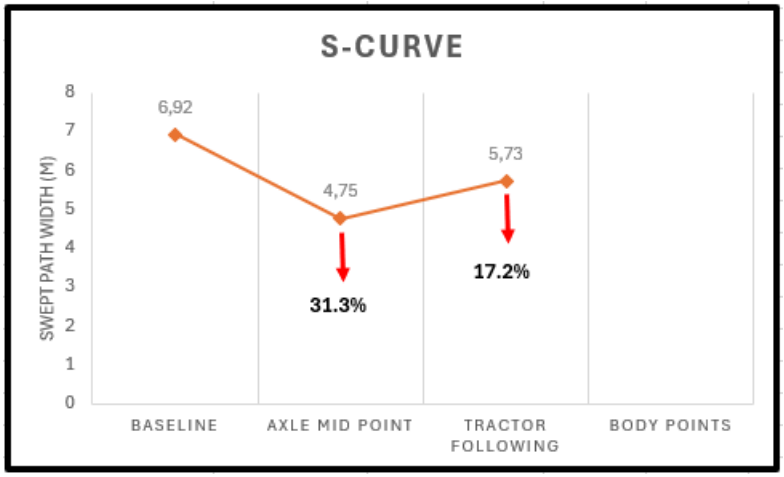

Figure 4.7: Performance of cost functions for a S-Shape maneuver of radius 20m.

4.1.2 Kinetic Results

4.1.2.1 No Dolly Steering

Figure 4.8 below illustrate the behavior of a vehicle when the steering control is not optimized, including the effects of dolly steering. Using the kinetic model, we analyzed the forces and yaw rates acting on each unit. A common observation is that the end of the maneuver is not smooth due to relaxed constraints, which simplifies the solution process. As shown in Figure 4.8c, the lateral force on units 2 and 4 are notably high because they carry heavy loads. Since the maneuver is performed at low speed, the yaw rates of each unit aim to achieve steady state due to constant steering. It's important to note that without dolly steering, the last unit is responsible for creating a high swept path width of 5.09m, which affects the vehicle's overall maneuverability. This insight highlights the significance of optimizing steering controls to improve vehicle performance.

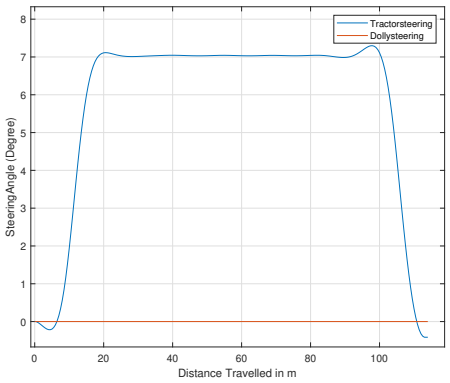

(a) Steering angle inputs

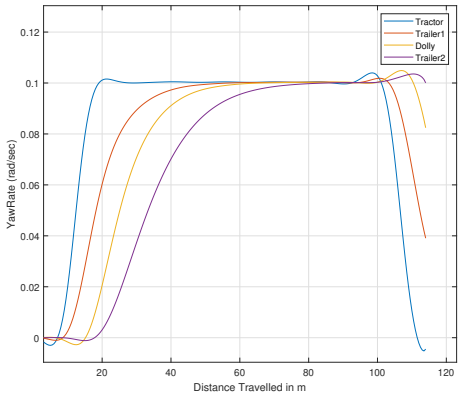

(b) Yaw rate outputs

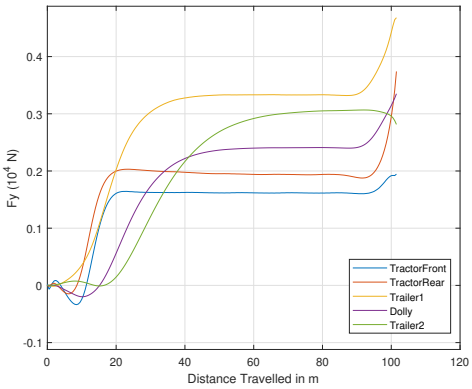

(c) Lateral force acting on each units

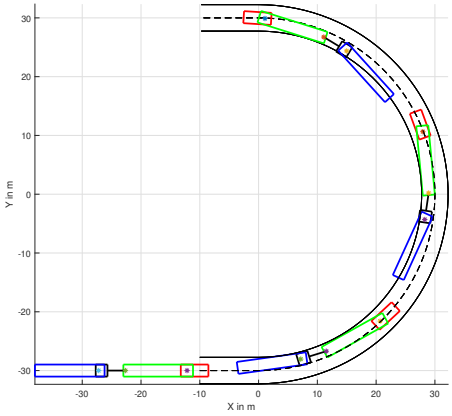

(d) Vehicle trajectory

Figure 4.8: No dolly steering for 180 degree maneuver

4.1.2.2 Dolly Steering - Axle Mid-point

The plots below illustrate the vehicle's behavior with optimized steering allocations for both the tractor and dolly. With the dolly steering, there is a noticeable non-zero steering input in Figure 4.9a, leading to higher yaw rates and lateral forces, as shown in Figures 4.9b and 4.9c respectively. These forces stabilize as the steering input stabilizes, ultimately reducing the vehicle's swept path to 3.87m. Among the three cost functions tested, the axle midpoint cost function provided the best results for safety and maneuverability. Additionally, this optimized setup enhances overall vehicle control and efficiency during maneuvers.

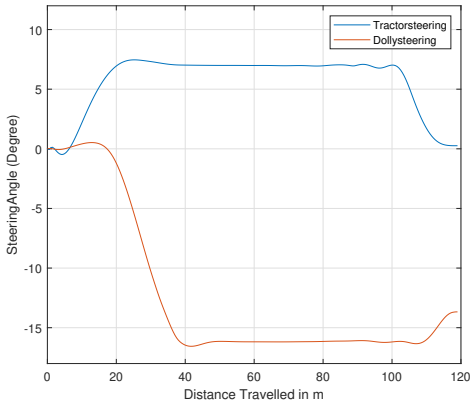

(a) Steering angle inputs

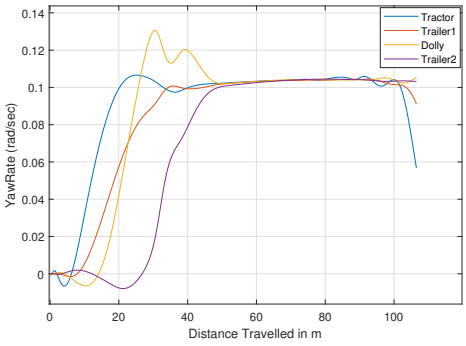

(b) Yaw rate outputs

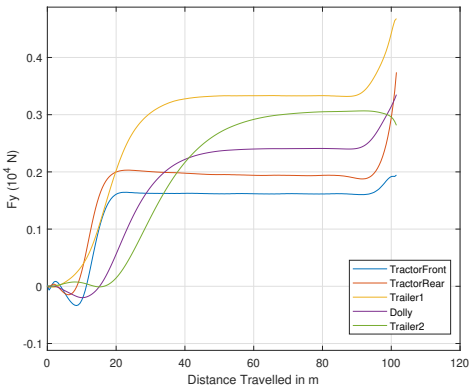

(c) Lateral force acting on each units

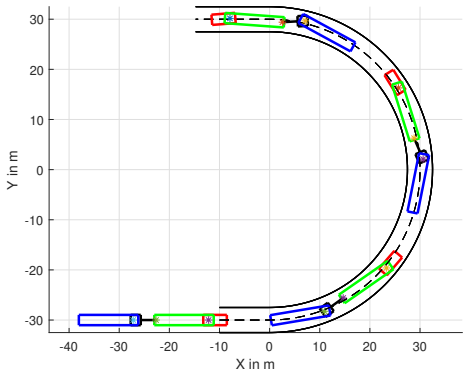

(d) Vehicle trajectory

Figure 4.9: Optimized dolly steering for 180 degree maneuver

The results above indicate that the overall performance of the A-double combination using a steerable dolly, particularly for a 180-degree maneuver, is consistent regardless of the vehicle model used. Specifically, the swept path width and the steering angle values that produced this width are comparable across different models. However, to avoid making premature conclusions, we also investigated the performance for other maneuvers to ensure comprehensive analysis. This approach ensures a thorough understanding of the vehicle's behavior across various scenarios.

4.2 Comparison between Kinematic Model and Kinetic Model

In this section, we will investigate and compare the results of optimizing steering input using two different vehicle models (kinematic and kinetic) for various maneuvers at low speeds. To ensure a fair comparison, we will primarily focus on the steering angles of the two units and the swept path created by the vehicle. This detailed comparison will help us understand the strengths and limitations of each model in

optimizing vehicle control.
Starting with the 90-degree maneuver, Figures 4.10a and 4.10b show the steering inputs and vehicle positions when using the kinematic model. Similarly, Figures 4.11a and 4.11b depict these characteristics when using the kinetic model. Although the steering input for the kinetic model is not smooth due to the high computational demands and time-consuming nature of solving the optimization problem, the results are still comparable. The swept path widths achieved after using different cost functions are compared for both kinematic and kinetic model in the table of comparison provided in Figure 4.14. Notably, during tighter turns, the vehicle tends to move outside the path before making the turn, a behavior observed with both models. This demonstrates the solver's effectiveness in finding optimal solutions for the given problem.

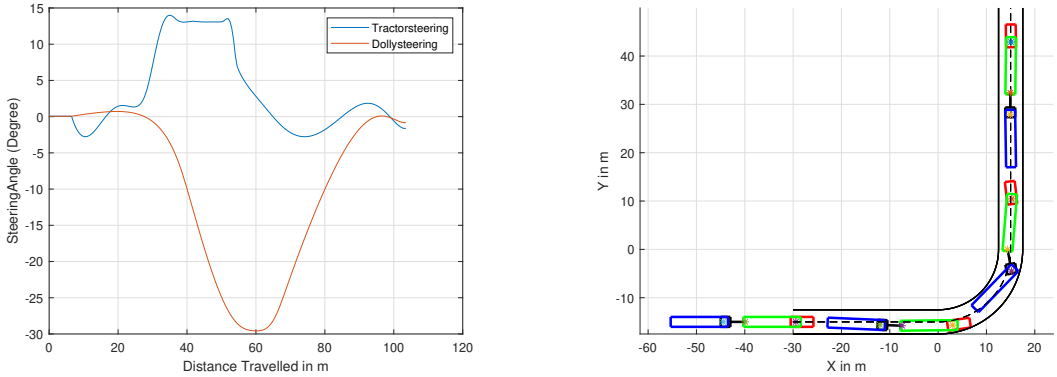

(a) Steering angle inputs **(b)** Vehicle trajectory

Figure 4.10: Optimal steering allocation using kinematic model for 90 degree turn

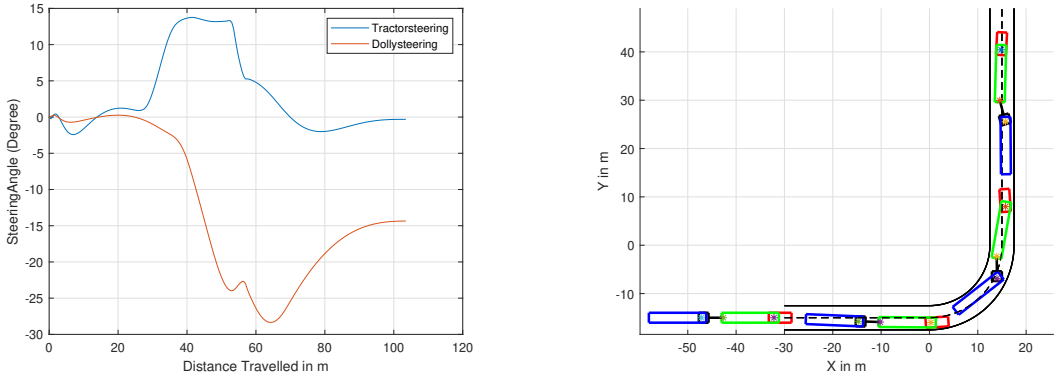

(a) Steering angle inputs **(b)** Vehicle trajectory

Figure 4.11: Optimal steering allocation using kinetic model for 90 degree turn

Moving to the S-curve maneuver, the comparison is similar to the 90-degree curve. Once again, the kinetic model did not produce as smooth results, but the outcomes from both models are similar, refer to Figures 4.12 and 4.13. For this maneuver,

which required the most instances to optimize, the unit distance for each instance was larger and fixed to save time. Additionally, strict constraints were removed. Despite these adjustments, the trajectories obtained from both models are almost identical, demonstrating their effectiveness in handling complex maneuvers.

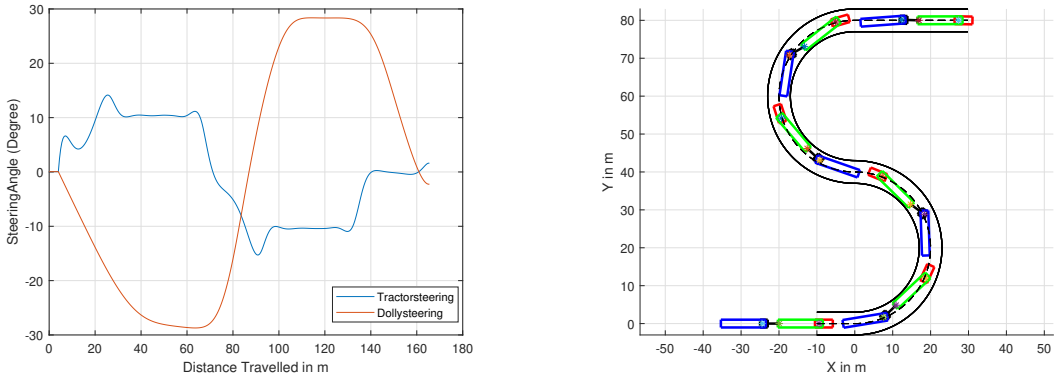

(a) Steering Angle Inputs **(b)** Vehicle Trajectory

Figure 4.12: Optimal steering allocation using kinematic Model for S curve

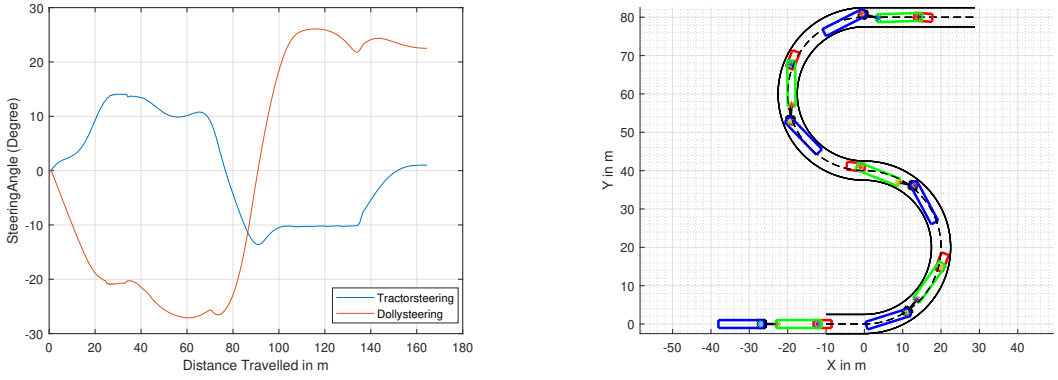

(a) Steering Angle Inputs **(b)** Vehicle Trajectory

Figure 4.13: Optimal steering allocation using kinetic Model for S curve

The comparison Table 4.14 summarizes all the results obtained using different cost functions when two different vehicle models were employed across various maneuvers. Although, some data is missing, as the solver either failed to find a solution or exceeded the anticipated number of iterations during optimization.

MANOEUVRE	COST FUNCTION	SWEPT PATH WIDTH (m)	
		Kinetic Model	Kinematic Model
180 deg Curve	No Dolly Steering	5.1	5.1
	Axle Mid Point	3.9	3.8
	Body Corner Point	3.8	3.7
	Tractor Following	3.8	3.9
90 deg. Curve	No Dolly Steering	7.4	7.4
	Axle Mid Point	5.1	5.3
	Body Corner Point	4.5	4.6
	Tractor Following	5.5	5.9
S Curve	No Dolly Steering	6.7	6.7
	Axle Mid Point	4.7	4.5
	Body Corner Point	5.7	5.3
	Tractor Following	5.02	-

Figure 4.14: Comparison of Swept path values for Kinematic and Kinetic models at low speeds

4.3 Objective 2 Reflection - Minimizing Off-Tracking

Minimizing off-tracking at high speeds involves complex interactions between various dynamic forces acting on the vehicle. By utilizing a kinetic model and evaluating good cost function, it is possible to optimize the objective that significantly improve vehicle stability, handling, and safety during high-speed maneuvers.

4.3.1 High Speed Off-Tracking

Below in LCV, where only the tractor's front axle is steered and the dolly is not, the yaw rate exhibits distinct phases as the vehicle negotiates a curve, evident in Figure 4.15b . As the combination enters the curve, the steering angle of the tractor's front axle increases sharply, leading to a sudden spike in yaw rate. This spike is more pronounced in the rear units of the LCV due to their distance from the steering axle and hence creating higher lateral deviation on dolly and second trailer with respect to tractor's axle midpoint, as evident in Figure 4.16. During the long turn, the yaw rate stabilizes as the steering angle holds steady. Upon exiting the curve, the steering angle decreases, causing the yaw rate to drop rapidly as the vehicle realigns with the straight path. This dynamic behavior highlights the challenges in maintaining stability and control in LCVs during high-speed maneuvers.
To optimize the performance in terms of stability and maneuverability, dolly steering was introduced alongside tractor steering. Two cost functions, axle mid-point and tractor following, were evaluated. When the dolly was steered in combination with

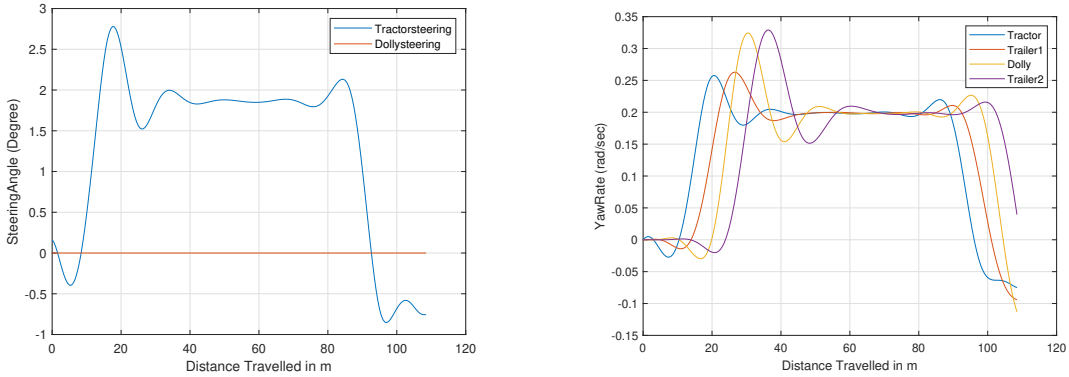

(a) Steering angle inputs **(b)** Yaw rate outputs

Figure 4.15: High speed off-tracking without optimization

the tractor, along with the off-tracking, the yaw rate amplification was significantly reduced, leading to a smoother region of steady-state yaw rate, as shown in Figure 4.17b. This indicates that the objective of minimizing lateral off-tracking also minimizes yaw amplification, as the dynamics of the vehicle show interrelated effects on these objectives. Steering angles of both steerable units, as shown in Figure 4.17a, were in the same direction, effectively counteracting the centrifugal force and dragging the last unit inward. This coordinated steering reduced lateral off-tracking, as illustrated in the trajectory of the combination's improved performance, as shown in Figure 4.17.

Figure 4.18 below illustrates the overall reduction in off-tracking for each unit relative to the tractor, compared to using two distinct cost functions. Notably, the cost function based on the axle midpoint resulted in a greater reduction in off-tracking compared to the tractor-following cost function. This is because the former provided the tractor with slightly more steering freedom, allowing for optimized steering for both the tractor and dolly. In contrast, the latter cost function focused solely on optimizing the dolly's steering.

4.4 Objective 3 Reflection - Minimizing Rearward Amplification

To achieve the objective of reward amplification using different cost functions, no maneuver is more effective than a lane change. This maneuver effectively tests the vehicle's stability, handling, and responsiveness under dynamic conditions. The lane change requires precise control and coordination of steering inputs, making it an ideal scenario for evaluating and optimizing the performance of an LCV with both tractor and dolly steering.

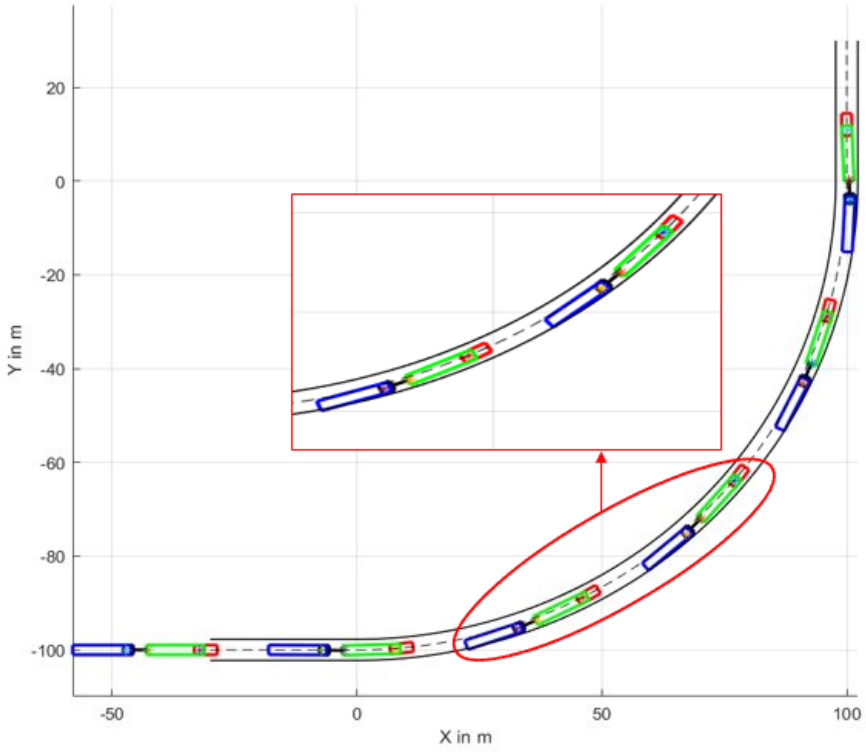

Figure 4.16: Vehicle trajectory without dolly steering - higher off-tracking

4.4.1 Lane Change

4.4.1.1 Single Lane Change

Starting with a single lane change maneuver, the vehicle's performance is evaluated based on its response to a sudden steering input while traveling at 80 km/h. This maneuver is defined by the vehicle's ability to follow a desired path through a controlled steering input at the tractor's front axle. Figure 4.20b of the yaw rate plot illustrates the dynamics of this maneuver, showing that the last two units of the combination experience a significantly higher yaw rate compared to the tractor. The amplification is even more pronounced when all units are fully transitioned into the second lane, highlighting the challenge of maintaining stability and control during such maneuvers. This indicates that the yaw rate has amplified, with an amplification factor greater than 1, that is 1.55 and 1.69 for dolly and second trailer respectively.

When the dolly is steered in conjunction with the tractor, there is a significant reduction in yaw rate amplification. This factor was reduced by 36% and 31.3% for dolly and second trailer respectively. Such coordinated steering ensures better stability and control of the vehicle combination. The dolly's steering angle is typically in the opposite direction to that of the tractor and is higher in magnitude. This is to counterbalance the yaw forces acting on the last unit, thereby maintaining its yaw rate at a level similar to that of the tractor. As a result, the yaw rate of the entire vehicle combination in Figure 4.21b is more uniform, which reduces the overall yaw rate amplification.

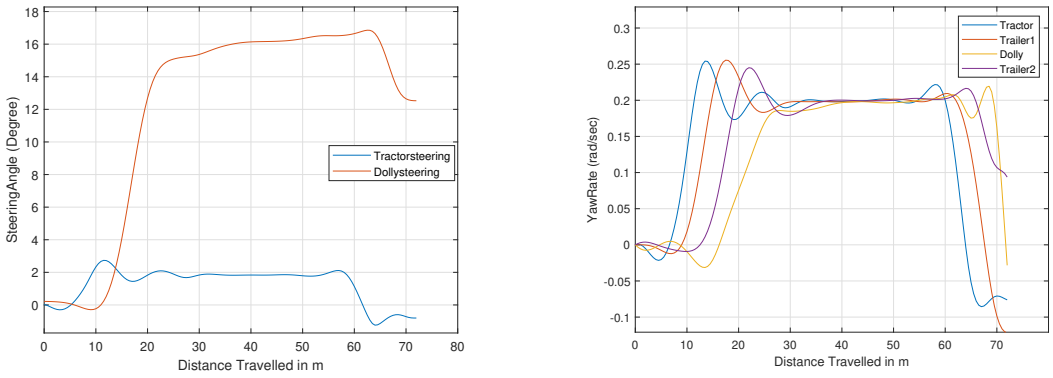

(a) Steering angle inputs **(b)** Yaw rate outputs

Figure 4.17: High speed off-tracking with optimization

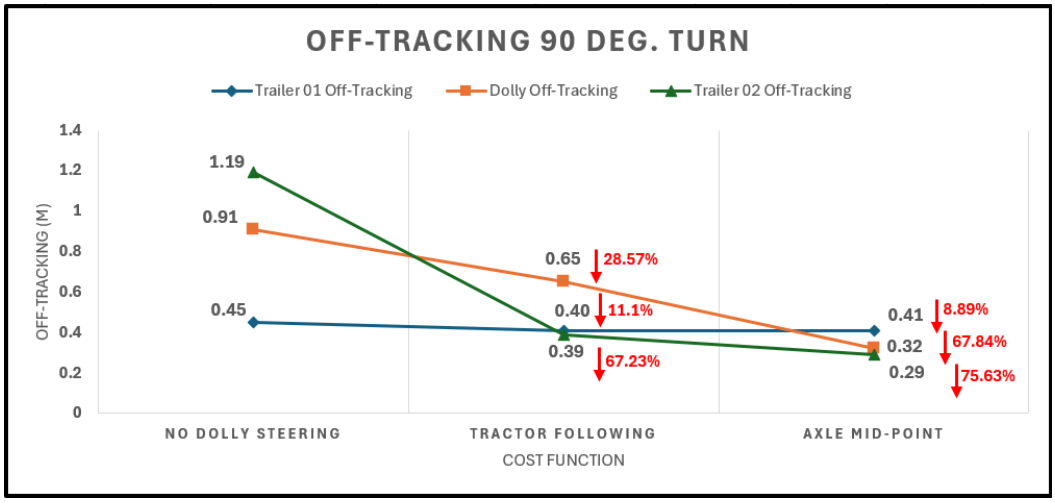

Figure 4.18: Performance of cost functions for reduction in off-tracking.

Figure 4.22 summarizes the reduction in the amplification factor for each unit. It is evident that, since the steering of the tractor was fixed in both steered and non-steered dolly vehicle combinations, there is no change in amplification for the first trailer. However, if the dolly were also propelled, it might have some effect on this factor.

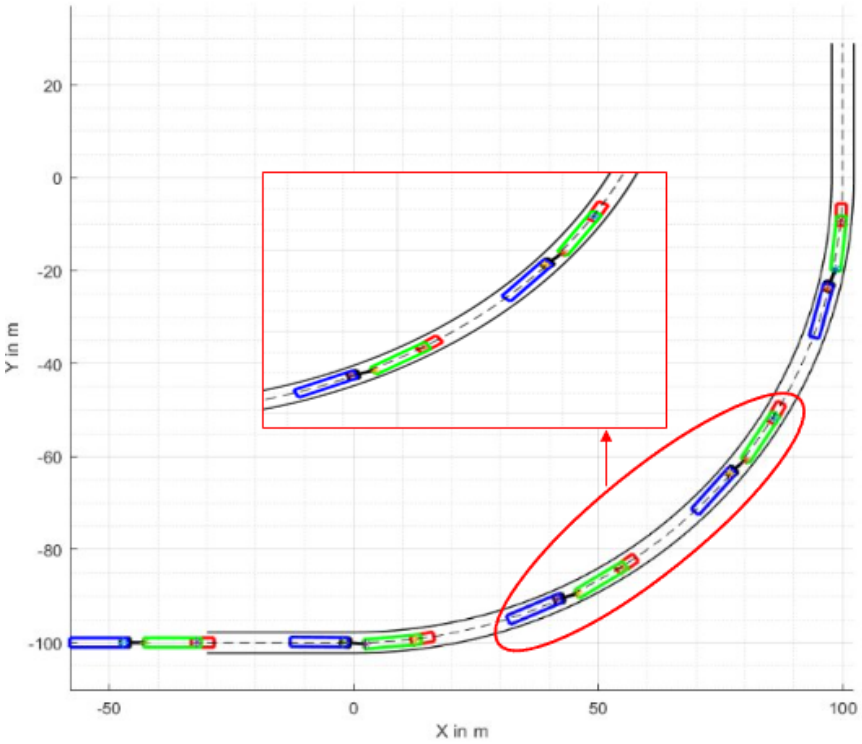

Figure 4.19: Vehicle trajectory after optimisation - reduced off-tracking

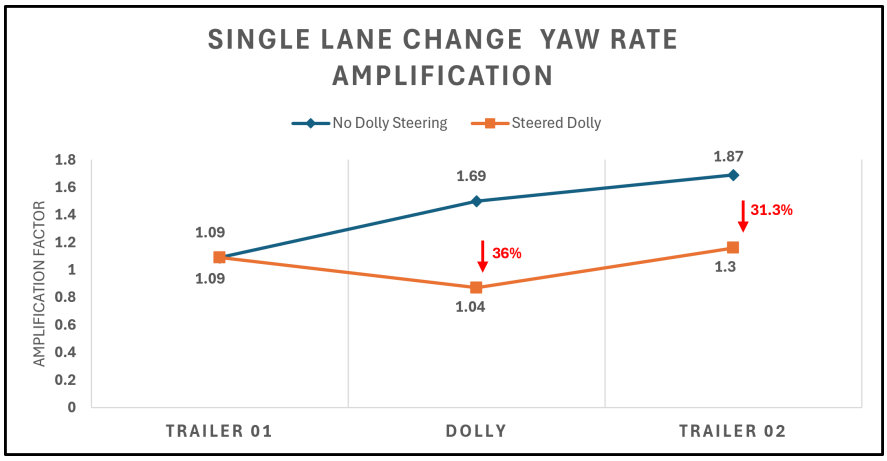

Figure 4.22: Reduction in rearward amplification for single lane change with dolly steering

4.4.1.2 Double Lane Change

To further test the maneuverability and stability of the vehicle combination using optimized control allocation for yaw rate amplification reduction, a double lane change maneuver is performed.
The plot in Figure 4.23a below illustrates the front axle tractor steering angle, which exhibits a sinusoidal pattern due to the vehicle needing to steer twice. This complex maneuver imposes additional challenges on vehicle dynamics, as it requires rapid and

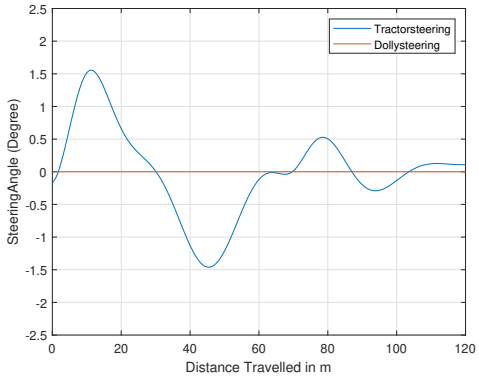

(a) Steering angle inputs

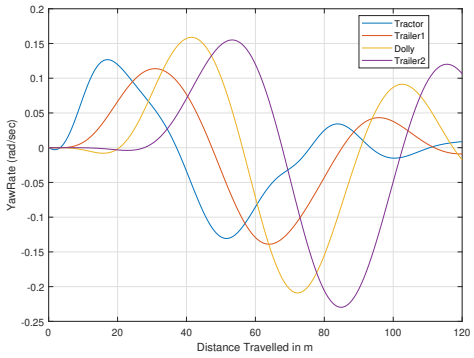

(b) Yaw rate outputs

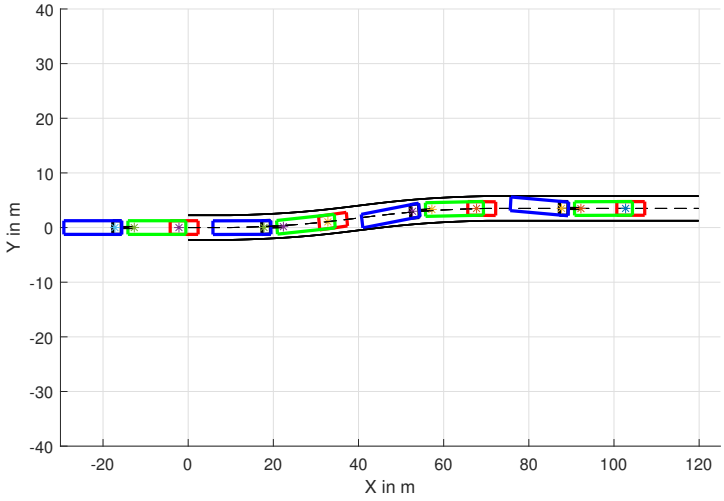

(c) Vehicle trajectory

Figure 4.20: Rearward amplification in single lane change when dolly is not steered

precise steering adjustments to maintain the desired path. As a result, the yaw rate experienced by the last two units of the combination is significantly higher, especially when the vehicle exits the curve. The yaw rate amplification factor for dolly and second trailer was observed to be 1.69 and 1.85 respectively. The rapid steering inputs and the necessity to change lanes twice amplify the yaw rate, indicating that the vehicle's stability is heavily tested under these conditions.
The amplified yaw rate highlights the importance of optimized control strategies to ensure that the last units of the combination can follow the tractor with minimal yaw rate discrepancies, thereby enhancing overall stability and maneuverability. Hence, when dolly steering is added to the vehicle combination, there is a significant reduction in yaw amplification for the dolly and trailer 2, by 38.4% and 30.4%, respectively, as shown in the figure. The synchronized steering between the tractor and dolly ensures that the yaw forces are better managed throughout the entire combination.

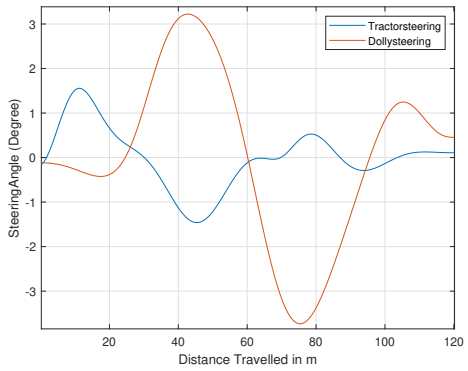

(a) Steering angle inputs

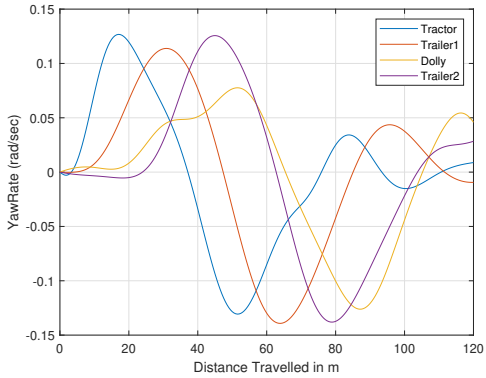

(b) Yaw rate outputs

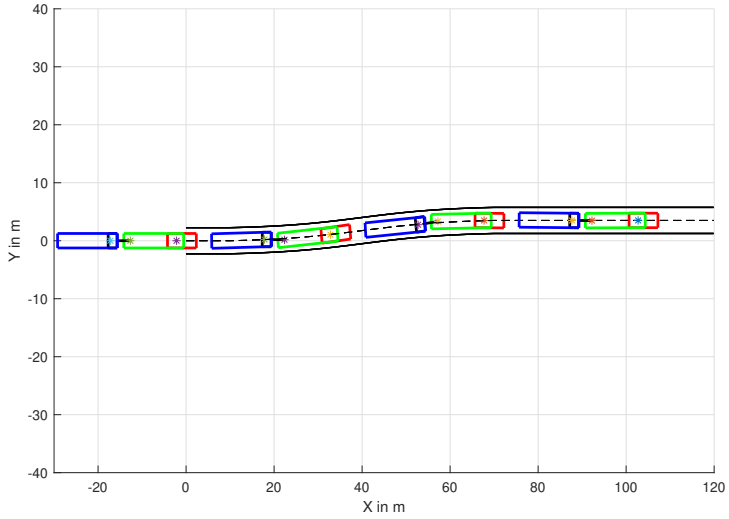

(c) Vehicle trajectory

Figure 4.21: Rearward amplification in single lane change when dolly is steered optimally

4.4.2 Dolly with steerable and propelled axle

In previous sections, we discussed how the integration of a steerable dolly axle in an LCV effectively reduces swept path, offtracking, and rearward amplification. We then explored the potential benefits of enhancing this configuration by adding propulsion to the dolly axle, making it not only steerable but also capable of self-propulsion.

The addition of propulsion to the steerable dolly axle is expected to improve control over both the dolly and the trailing second trailer, especially during high-speed maneuvers. To test this hypothesis, we conducted an optimization analysis focusing on a high-speed 90-degree turn, using a dolly axle equipped with both steering and propulsion capabilities. The primary objective was to assess the impact of this

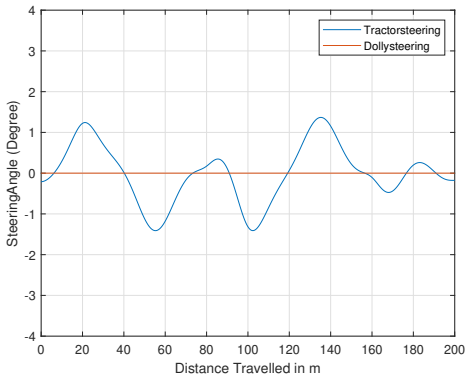

(a) Steering angle inputs

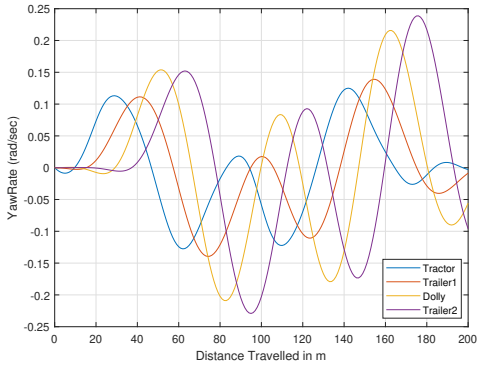

(b) Yaw rate outputs

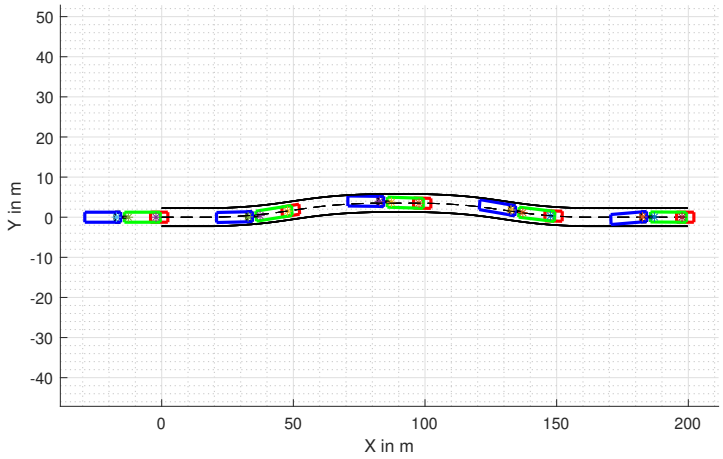

(c) Vehicle trajectory

Figure 4.23: Rearward amplification in double lane change when dolly is not steered

configuration on reducing offtracking and yaw amplification.

The comparative results, illustrating the reduction in high-speed offtracking when using a steerable dolly versus a dolly with both steering and propulsion, are presented in Figure 4.27.

From the plot in Figure 4.27, it's evident that while a dolly equipped with both steering and propulsion does reduce off-tracking compared to a non-steered dolly, the improvement does not surpass the benefits observed with a dolly that has a steerable axle alone. The potential for enhanced maneuverability through the use of a propelled axle would likely be greater if differential braking capabilities were available, allowing independent control of the propulsion forces on the left and right wheels. However, this optimization falls outside the scope of our current single-track model.

When examining the trajectory of the LCV shown in Figure 4.28, and comparing it with the trajectory of the LCV equipped with only a steerable axle (as seen in Figure 4.19), it is evident that the LCV with the additional capabilities adheres more effectively to the road boundaries. Specifically, it maintains a greater distance

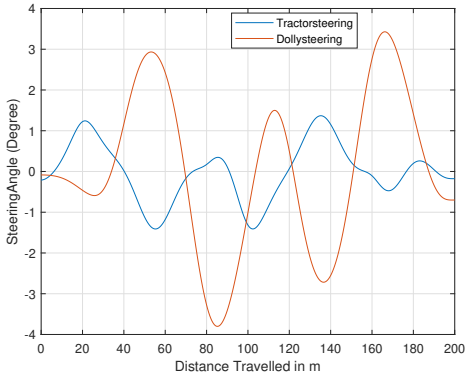

(a) Steering angle inputs

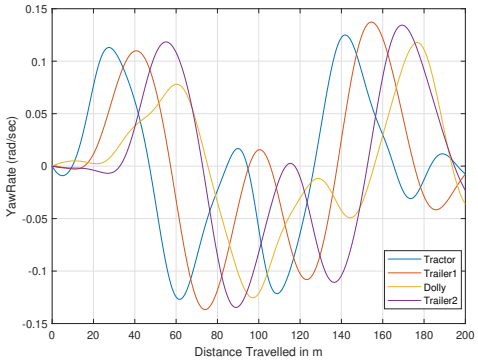

(b) Yaw rate outputs

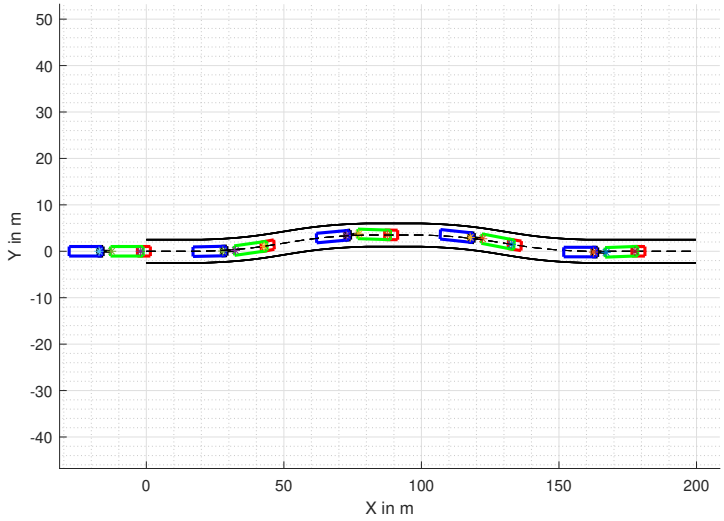

(c) Vehicle trajectory

Figure 4.24: Rearward amplification in double lane change when dolly is steered optimally

from the road edges, demonstrating a more substantial compliance with the road limits at higher speeds.

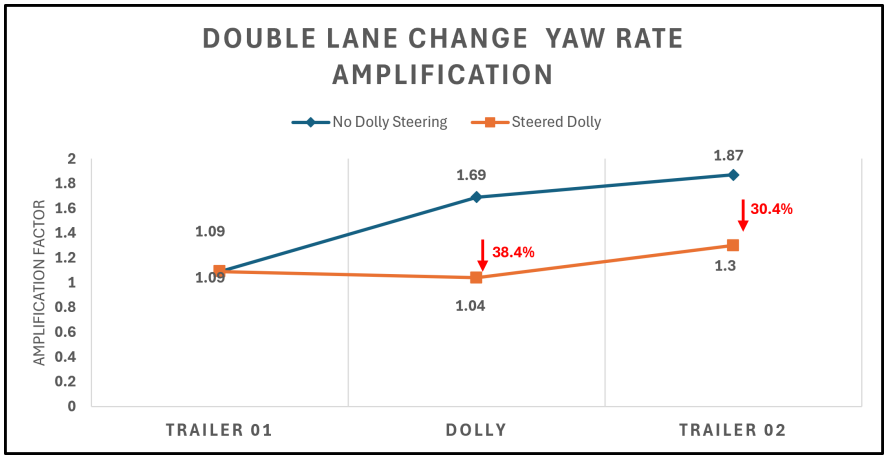

Figure 4.25: Reduction in rearward amplification fo double lane change with dolly steering.

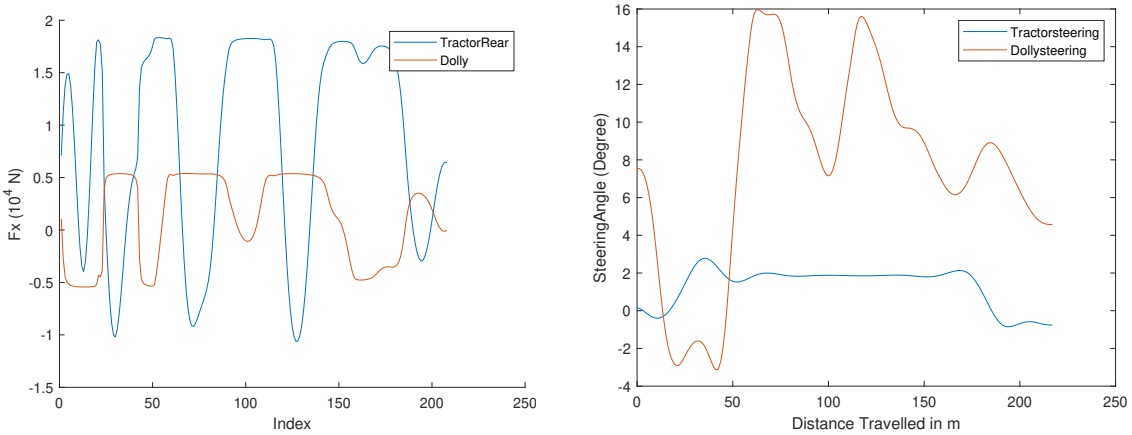

(a) Propulsion forces **(b)** Steering angles

Figure 4.26: Rearward amplification in double lane change when dolly is steered optimally

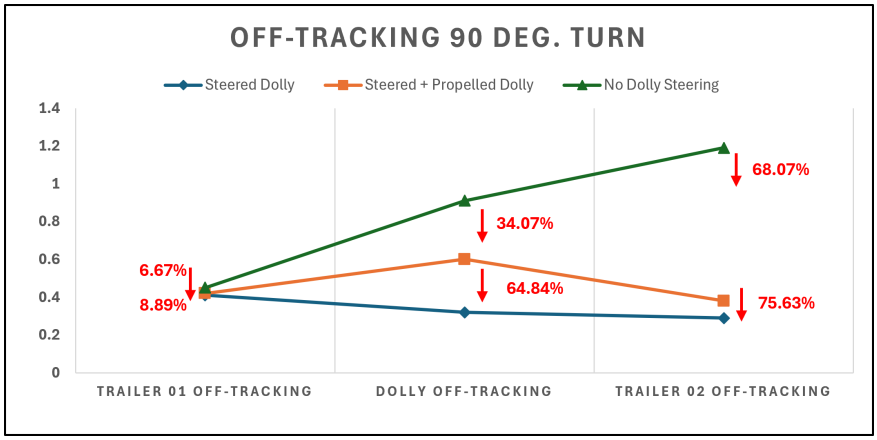

Figure 4.27: Performance comparison for reduction in off-tracking using a propelled dolly.

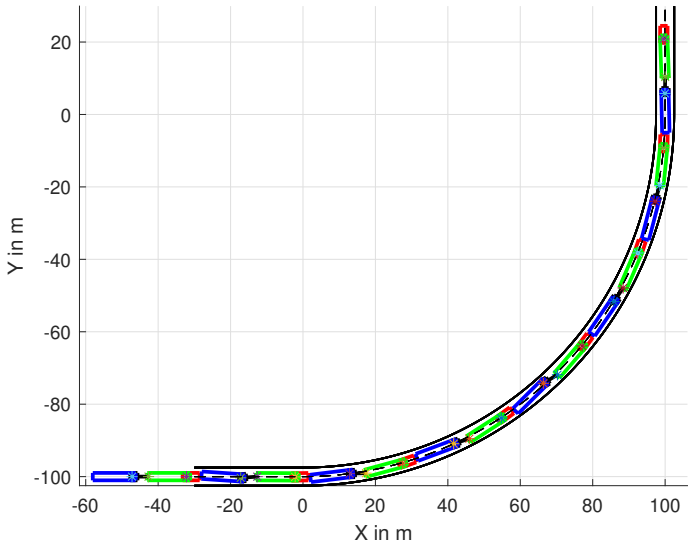

Figure 4.28: Vehicle trajectory for LCV with steered and propelled dolly axle.

5
Conclusion

This thesis work proposes an optimal steering control strategy for the tractor and dolly of an A-double combination. This strategy significantly enhances stability, maneuverability, and safety across various driving scenarios. The optimization methods and cost functions utilized in this study can also be adapted for use in other long vehicle combinations with steerable axles.

Two types of vehicle models were employed in this work: kinematic and kinetic, each offering distinct advantages for optimization purposes. The kinematic model is highly effective for finding optimal solution in less time for low-speed maneuvers. Its simplicity allows for faster computations, which is especially beneficial when the number of units in the vehicle combination increases. This model simplifies the control process without compromising the ability to plan and execute precise maneuvers. The kinetic model becomes essential when considering scenarios where vehicle dynamics significantly impact stability and maneuverability. This model incorporates the forces and moments acting on the vehicle, providing a more accurate representation of its behavior at higher speeds or during complex maneuvers. As shown in the results section, both models produced nearly similar outcomes, so the choice between them depends on the maneuver characteristics and computational cost.

The use of a single cost function allows the optimization process by addressing multiple objectives simultaneously. Since these objectives (off-tracking, yaw-amplifications) are interconnected, a unified cost function can efficiently balance them without the need for separate optimization criteria. Overall, the cost function axle mid-point performed well compared to others in terms of achieving multiple objectives in various maneuvers. As it gives freedom to every steerable multiple units The optimal control strategies can assist human drivers in maintaining control and stability, especially in challenging situations. And for autonomous vehicles too, ensuring the objectives are met and vehicle follows the desired path. The process could be extended to reverse parking of LCVs, where precise control and maneuverability are crucial. In vehicles with multiple steerable axles, there is a risk of overactuation, where too many control inputs can lead to inefficiencies or conflicts. The proposed optimization method effectively manages this by coordinating the actions of all steerable axles, ensuring smooth and efficient control. As optimization was performed considering the path distance domain rather than time-controlled actions. This approach is advantageous in scenarios where the vehicle may come to a halt, as it eliminates dependency on time-based controls.

6

Discussion

In this section we try to delve into the possible solutions and scenarios on how these cost functions can be implemented in a real time scenarios and be able to perform optimal control allocation.

6.1 Real-Time Implementation

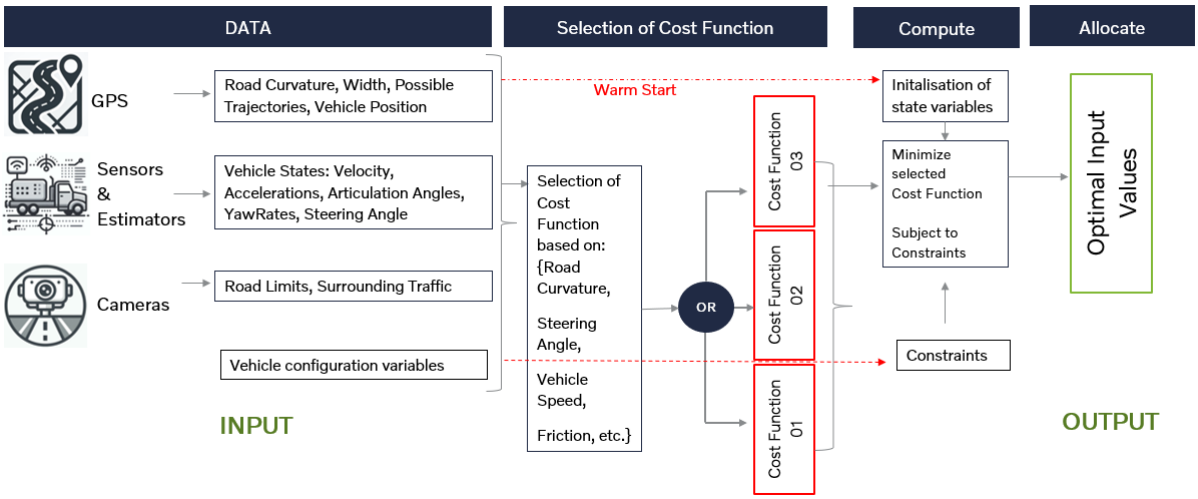

Figure 6.1: Flowchart for real-time implementation.

As seen in the above figure, we can look at the implementation of the cost function in real time by addressing the four different phases.

1. Input Data: The input data for the cost function is the curvature of the road ahead, estimated and measured vehicle states, vehicle configuration variables and data about the surrounding environment such as available path and road limits.
2. Selection of Cost Function: Once we have the data on road curvature and possible maneuverability options, the system will be able to choose the most suitable cost function for the scenario.
3. Computation: After the selection of cost function is done, the optimisation function is evaluated online to compute the optimal control inputs for the different actuators for the upcoming scenario.

4. Allocation: Now, that the system has the computed values for the desired maneuverability. The control inputs are allocated once the vehicle unit reaches, the particular point in the path for which the optimal input was computed.

6.1.1 Collection and usage of Input Data

The input data for the control algorithm can be collected from multiple types of sensors and estimators. For the data of road curvature we use the GPS and satellite map data and route map being used. From this road curvature data, the system will be able to compute the cost function for the section of the path ahead of time and keep the optimal control inputs ready for allocation once the vehicle unit reaches that desired point in the path.

From the path data, the system will also be able to initialise data for estimated vehicle states like yaw angles, position and speed. This data can be supplied to the optimisation algorithm as a warm start to improve computation speed. In addition to this the sensors and estimators onboard the vehicle are also used for information of current vehicle state and other vehicle configuration variables like mass, cog position etc. which is used to determine the constraints like limiting lateral acceleration to avoid unsafe modes.

In addition to the above, camera data is also used to limit actuation if necessary based on surrounding environment conditions.

6.1.2 Selection of cost function

From the initial evaluation of cost functions for different maneuvers, it is evident that a certain cost function can be more suitable for a particular maneuver, so real time computation and comparison of this cost functions online will make it possible to implement the best performing cost function or based on pre-defined maneuver conditions cost function selection can be carried out online.

6.1.3 Implementation of Optimal Input

Once the optimally allocated control inputs are computed, the input signals can be sent to the actuators once the unit combination reaches a desired location on the path for which the control input was computed.

6.2 Future Scope

The strategy to optimally control multi-trailer vehicles can be significantly expanded by increasing the number of actuators, not only for steering but also for propulsion. Further investigating more cost functions and employing improved vehicle model, consequently opens up numerous possibility for further research. The following points outline potential areas of investigation:

1. Advanced vehicle model: The vehicle model used in this thesis can be upgraded to a multi-track model with a non-linear tire model. This improvement will enable a more accurate representation of vehicle dynamics, closely resembling the behavior of actual vehicles.
2. Torque vectoring: Utilizing a multi-track model provides the opportunity to investigate different propulsive forces on either side of the vehicle. This can help in active steering by distributing torque optimally across the wheels.
3. Propulsion on trailer: Researching the effects of adding propulsion systems to trailers can bring insights into better vehicle handling and energy management.
4. Implementation in VTM: The optimal actuation strategy developed can be implemented and tested in high fidelity model (VTM) to evaluate its real-world effectiveness.

Bibliography

[1] Lynn De Smedt and Frederic De Wispelaere. Road freight transport in the eu. 2020.

[2] High capacity transport smarter policies for smart transport solutions. *ACEA Auto*, 2019.

[3] *International Transport Forum (ITF)*, 2021.

[4] Theodor Westny Carl Hynén Ulfsjöö. Modeling and lateral control of tractor-trailer vehicles during aggressive maneuvers. 2020.

[5] Bengt Jacobson. Vehicle motion engineering compendium, chalmers university. 2023.

[6] Maliheh Sadeghi Kati. Definitions of performance based characteristics for long heavy vehicle combinations. 2013.

[7] Mansour Keshavaraz Bahaghighat. Yaw and lateral predictive control in long combinations of heavy vehicles.

[8] Karin Uhlen, Per Nyman, Johan Eklöv, Leo Laine, Maliheh Sadeghi Kati, and Jonas Fredriksson. Coordination of actuators for an a-double heavy vehicle combination using control allocation. 2014.

[9] Toheed Ghandriz, Bengt Jacobson, Peter Nilsson, Leo Laine, and Niklas Fröjd. Computationally efficient nonlinear one-and two-track models for multitrailer road vehicles. 2020.

[10] Joris Gillis Greg Horn James B. Rawlings Andersson, Joel AE and Moritz Diehl. Casadi: a software framework for nonlinear optimization and optimal control. *Mathematical Programming Computation 11, no. 1.*

[11] Australian National Transport Commission. Performance-based standards scheme – the standards and vehicle assessment rules.

A

Appendix 1

Lorem ipsum dolor sit amet, consectetur adipisicing elit, sed do eiusmod tempor incididunt ut labore et dolore magna aliqua. Ut enim ad minim veniam, quis nostrud exercitation ullamco laboris nisi ut aliquip ex ea commodo consequat. Duis aute irure dolor in reprehenderit in voluptate velit esse cillum dolore eu fugiat nulla pariatur. Excepteur sint occaecat cupidatat non proident, sunt in culpa qui officia deserunt mollit anim id est laborum.

DEPARTMENT OF MECHANICAL AND MARITIME SCIENCES
CHALMERS UNIVERSITY OF TECHNOLOGY
Gothenburg, Sweden
www.chalmers.se

CHALMERS
UNIVERSITY OF TECHNOLOGY